ÅBO AKADEMI

INSTITUTIONEN FÖR
KEMITEKNIK

DEPARTMENT OF CHEMICAL
ENGINEERING

Processkemiska centret

Process Chemistry Centre

REPORT 12-03

Corrosion behaviour of boiler tube materials during combustion of fuels containing Zn and Pb

Dorota Bankiewicz

Academic Dissertation

Laboratory of Inorganic Chemistry

Corrosion behaviour of boiler tube materials during combustion of fuels containing Zn and Pb

Dorota Bankiewicz

Academic Dissertation

Laboratory of Inorganic Chemistry
Process Chemistry Centre
Department of Chemical Engineering
Åbo Akademi University

Supervisors

Professor Mikko Hupa
Åbo Akademi University
Department of Chemical Engineering
Turku, Finland

D. Sc. Patrik Yrjas
Åbo Akademi University
Department of Chemical Engineering
Turku, Finland

Opponent and Reviewer

Professor Kim Dam-Johansen
Technical University of Denmark
Department of Chemical and Biochemical Engineering
Lyngby, Denmark

Reviewer

D. Sc. Keijo Salmenoja
Andritz Oy
Recovery & Power Division
Helsinki, Finland

ISSN 159-8205
ISBN 978-952-12-2746-2 (paper version)
ISBN 978-952-12-2747-9 (pdf version)

Printing by Painosalama Oy

Åbo, Finland, 2012

"I always knew I would look back at the times we cried and laugh but
I never knew I would look back at the times we laughed and cry"
- Unknown

To Marcin Lichnowski (1981 – 2007)
– the best friend, passionate and outstanding person.
Thank you for giving me energy, support, hope and for showing me
better sides of life. You will be always in my heart!

Preface

The work described in this thesis was carried out at the Laboratory of Inorganic Chemistry at Åbo Akademi University as a part of the activities of the Process Chemistry Centre during 2007-2012. I gratefully acknowledge the assistance without which this research would not have been possible: three years of funding from the INECSE-Marie Curie Early Stage Training Programme, financial support from the Process Chemistry Centre at Åbo Akademi University and from the ChemCom and FUSEC projects. I also wish to acknowledge the financial support from the Stiftelsen för Åbo Akademi that enabled me to participate at a conference.

I would like to express my sincere appreciation to Prof. Mikko Hupa for the opportunity to be a part of the group, for his understanding, kindness and continual support, both intellectual and financial, what have been vital during the long journey of my doctoral studies. The greatest thanks go to my day-to-day supervisor D. Sc. Patrik Yrjas for his outstanding patience and for his trust. Thank you for giving me a free hand in my research and for helping me grow in confidence. I also want to thank Docent Bengt-Johan Skrifvars for taking good care of me at the beginning of my studies and for helping me acquire my passion for corrosion.

Without the help of two people in particular the chance of studying at Åbo Akademi University would have passed me by. I therefore wish to express my warm thanks to Docent Edgardo Coda Zabetta and to Prof. Wojciech Nowak for their help, including their always open-minded and encouraging attitude that opened up new possibilities for me.

During my studies I had the opportunity to spend four months in Germany at the Technical University of Munich (Institute of Energy Systems). This was a highly productive time. I would like to thank Prof. Hartmut Spliethoff for hosting me. Special thanks go to Dr.-Ing. Elisa Alonso-Herranz (one of my co-authors) for her selfless collaboration during our long test days and nights. Eli it was a great experience to work with you. I would also like to mention Rastko Jovanovič, Senthoorselvan Sivalingam and Christoph Wieland who made my stay in Munich unforgettable.

I have found the help of all my co-authors invaluable. There are three people however whom I was constantly bothering with my questions and I would like to thank them in particular D. Sc. Sonja Enestam – thank you Sonja for sharing with me your industrial experience which showed the Zn-Pb picture from a totally different side. You showed me the importance of this research and your reassurance about its relevance encouraged me at the most critical moments. Thank you for involving me in the boiler inspection, for your inspirational attitude and pleasing collaboration. D. Sc. Pasi Vainikka – Pasi the work done with you was a pure pleasure. You always knew how to motivate me and how to argue our work. Thank you for the great support and inspiration you gave me during our collaboration. D. Sc. Daniel Lindberg – Daniel your knowledge and willingness to share it with everyone who needs it makes thermodynamics more interesting that one can imagine. Thank you for the time you

spent explaining to me what had seemed incomprehensible and for calculating phase diagrams and T_0's for all the mixtures that came to my mind.

Further, I would like to express my special gratitude by naming a few more people who have contributed in the development of this thesis in different ways. My first steps in the corrosion lab were under the supervision of Lic. Sc. Micaela Westèn, who taught me the whole corrosion method which I used and developed in my research. All the (thousands) SEM/EDX analyses done by Mr Linus Silvander are invaluable. Thank you Linus for your time, for always being ready to help (no matter if it was week day or Sunday) and continuously digging for me some old data. Ms Jaana Paananen has been my greatest laboratory support, the person of highest reliability without whose back up some corrosion projects would simply not have been done in time. Jaana you are an angel. Sincere thanks are extended to Ms Mia Mäkinen and Ms Eva Harjunkoski for their professional help and friendship and for being always in the right place at the right time. I thank also D. Sc. Nikolai DeMartini for his supportive attitude that means more than he probably realizes. Further, I thank the amazingly skilful men in the lab, especially D. Sc. Mikael Bergelin, whose help with building new laboratory test rigs was of great importance while I was working with different corrosion projects. I would also like to acknowledge Ms Johanna Tuiremo for all the discussions and for her valuable professional comments.

In general, I would like to thank all the members of the OOK group for their constant readiness to help that made for an exceptionally pleasant work atmosphere.

The final stages of the PhD were extremely hard for me. The deadlines, the struggling with the text, the loss of motivation and many doubts came to me unexpectedly and put me under considerable pressure. However, all those difficulties become minor when you have wonderful friends around you. There is a big group of important people around me in Poland, in Finland and in other countries. I don't need to name you all…You know exactly who you are and how much you mean to me. I would however like to express my special gratitude to those who have been giving me daily companionship both at work and outside office hours during the whole PhD period: Pati, Xiaoju, Grześ, Wika, Michał and Johan L …thank you for all these years, days and moments. You were always there ready to help, to laugh and to cry with me and you are in a way good spirits of this thesis. A particularly warm embrace goes to Pati for always 'being there'.

Finally, I would like to warmly thank my parents, especially my mother who has been more than a support through the whole my life. She knows what is of the most importance in life. She has never pushed me but let me live with my own choices. Mamka dziękuję za wszystko, co dla mnie zrobiłaś i robisz, że zawsze mnie rozumiesz i jesteś kiedy Cię potrzebuje! My whole family has given me its loving support. Dziękuję Wam!

Åbo, March 2012

Abstract

Many power plants burning challenging fuels such as waste-derived fuels experience failures of the superheaters and/or increased waterwall corrosion due to aggressive fuel components already at low temperatures. To minimize corrosion problems in waste-fired boilers, the steam temperature is currently kept at a relatively low level which drastically limits power production efficiency.

The elements found in deposits of waste and waste-derived fuels burning boilers that are most frequently associated with high-temperature corrosion are: Cl, S, and there are also indications of Br; alkali metals, mainly K and Na, and heavy metals such as Pb and Zn. The low steam pressure and temperature in waste-fired boilers also influence the temperature of the waterwall steel which is nowadays kept in the range of 300 °C - 400 °C. Alkali chloride (KCl, NaCl) induced high-temperature corrosion has not been reported to be particularly relevant at such low material temperatures, but the presence of Zn and Pb compounds in the deposits have been found to induce corrosion already in the 300 °C - 400 °C temperature range. Upon combustion, Zn and Pb may react with Cl and S to form chlorides and sulphates in the flue gases. These specific heavy metal compounds are of special concern due to the formation of low melting salt mixtures. These low melting, gaseous or solid compounds are entrained in the flue gases and may stick or condense on colder surfaces of furnace walls and superheaters when passing the convective parts of the boiler, thereby forming an aggressive deposit. A deposit rich in heavy metal (Zn, Pb) chlorides and sulphates increases the risk for corrosion which can be additionally enhanced by the presence of a molten phase.

The objective of this study was to obtain better insight into high-temperature corrosion induced by Zn and Pb and to estimate the behaviour and resistance of some boiler superheater and waterwall materials in environments rich in those heavy metals, including at increased temperatures of materials. Therefore, extensive laboratory, bench-scale and full-scale tests were carried out. The results from these tests may be directly made use of in practical applications, for example for screening steels from the materials selection, as well as in the development of corrosion preventing tools by finding corrosion initiating triggers and understanding their effect on high-temperature corrosion.

The laboratory study covered steel exposure tests with pure $ZnCl_2$, ZnO, $PbCl_2$ and PbO as well as with a number of salt mixtures: $ZnCl_2$-K_2SO_4, $PbCl_2$-K_2SO_4, $PbCl_2$-KCl and $PbCl_2$-$ZnCl_2$-KCl. It was shown that pure $PbCl_2$ starts to be aggressive to the low-alloy steel (10CrMo9-10) and also to the stainless steels (AISI 347) already at temperatures around 350 °C, below the melting temperature of $PbCl_2$ which is 501 °C. The protective Cr_2O_3 on the AISI 347 was destroyed due to $PbCrO_4$ formation. The exposures to $ZnCl_2$ showed an increased oxide layer growth on the 10CrMo9-10 already at 350 °C, but negligible oxide layer growth on the AISI 347 up to 450 °C. Above 350 °C, the fast evaporation of $ZnCl_2$ suppressed the growth of the oxide layer.

The tests with $ZnCl_2$- and $PbCl_2$-containing mixtures ($ZnCl_2$-K_2SO_4, $PbCl_2$-K_2SO_4, $PbCl_2$-KCl and $PbCl_2$-$ZnCl_2$-KCl) showed that the $ZnCl_2$-containing mixture ($PbCl_2$-$ZnCl_2$-KCl) was

more aggressive and active at lower temperatures than the $PbCl_2$-KCl mixture. It suggests, therefore, that $ZnCl_2$ is more likely to cause problems at lower material temperatures, while $PbCl_2$ is more stable and is expected to be problematic at both waterwall and superheater temperatures. At 400 °C, the highest corrosion rates on both test materials were observed when both $PbCl_2$ and $ZnCl_2$ were present in the salt. The $PbCl_2$-$ZnCl_2$-KCl mixture contained the highest fraction of melt out of all tested salt mixtures but the corrosiveness of this mixture was not the highest at all test temperatures. Thus, the amount of melt does not necessary decide the extent of corrosion. At 500 °C and above the corrosion caused by all three mixtures containing $PbCl_2$ was significant and both steels were damaged to a similar degree. The results from the tests with the mixtures containing 5 wt-% $PbCl_2$ were similar to the results from the tests with pure $PbCl_2$ showing its extremely corrosive character.

ZnO was shown not to be corrosive to the low-alloy steel (10CrMo9-10) and nor to the stainless steel (AISI 347) at 550 °C. The oxide layer thickness was comparable to the test with no salt present. However, tests with PbO at 550 °C caused a noticeable oxide layer growth on 10CrMo9-10 and fairly low on AISI 347.

To better understand the fate of Zn and its effect on high-temperature corrosion specifically in waste-wood fired fluidized bed boilers, high-temperature corrosion/deposit probe tests were performed in a 30 kW_{th} bubbling fluidized-bed reactor by firing wood pellets doped with $ZnCl_2$ to simulate waste wood. Specific issues of interest in this study included the general impact of firing waste wood containing higher amounts of Zn and Cl and the evaluation of the role of $ZnCl_2$ in high-temperature corrosion. The tests showed that the presence of $ZnCl_2$ had a clear impact on high-temperature corrosion of low-alloy steel. When compared to the combustion of pure wood pellet, corrosion increased at temperatures above 450 °C (probe cooling temperature). The K_2ZnCl_4 which was found in the deposit was concluded to be the main corrosive agent.

During the planning stage of further experiments there were strong indications of bromide induced high-temperature corrosion of the waterwalls. In consequence, a measurement campaign in a BFB co-combusting SRF was performed to determine the occurrence of corrosive Cl-, Br-, Zn- and Pb-compounds in the fuel, in the furnace vapours and in the waterwall deposits. The relative corrosiveness of chlorides and bromides was further established by means of laboratory experiments. A $ZnBr_2$-K_2SO_4 salt mixture was tested and compared with a corresponding $ZnCl_2$-K_2SO_4 salt mixture. The mixture with $ZnBr_2$ was found to be more aggressive at 400 °C in oxidising conditions than the corresponding mixture with $ZnCl_2$. A measurement campaign showed that vapours in the furnace were enriched with Cl and small amounts of Br, Zn and Pb. The chemical thermodynamic calculations indicated that possible forms of those compounds at the waterwall deposit temperatures (400 °C) were Na-, K-bromides and chlorides and Zn- and Pb-sulphides or sulphates in reducing and oxidizing conditions, respectively. The thermodynamic calculations correlated with the deposit analysis.

Svensk sammanfattning

Många förbränningsanläggningar som bränner utmanande bränslen såsom restfraktioner och avfall råkar ut för problem med ökad korrosion på överhettare och/eller vattenväggar pga. komponenter i bränslena som är korrosiva redan vid låga temperaturer. För att minimera problemen i avfallseldade pannor hålls ångparametrarna på en relativt låg nivå, vilket drastiskt minskar energiproduktionen.

Beläggningarna i avfallseldade pannor består till största delen av element som är förknippade med högtemperaturkorrosion: Cl, S, alkalimetaller, främst K och Na, och tungmetaller som Pb och Zn, och det finns också indikationer av Br-förekomst. Det låga ångtrycket i avfallseldade pannor påverkar också stålrörens temperatur i pannväggarna i eldstaden. I dagens läge hålls temperaturen normalt vid 300 - 400 °C. Alkalikloridorsakad (KCl, NaCl) högtemperaturkorrosion har inte rapporterats vara relevant vid såpass låga temperaturer, men närvaro av Zn- och Pb-komponenter i beläggningarna har påvisats förorsaka ökad korrosion redan vid 300-400 °C. Vid förbränning kan Zn och Pb reagera med S och Cl och bilda klorider och sulfater i rökgaserna. Dessa tungmetallföreningar är speciellt problematiska pga. de bildar lågsmältande saltblandningar. Dessa lågsmältande gasformiga eller fasta föreningar följer rökgasen och kan sedan fastna eller kondensera på kallare ytor på pannväggar eller överhettare för att sedan bilda aggressiva beläggningar. Tungmetallrika (Pb, Zn) klorider och sulfater ökar risken för korrosion, och effekten förstärks ytterligare vid närvaro av smälta.

Motivet med den här studien var att få en bättre insikt i högtemperaturkorrosion förorsakad av Zn och Pb, samt att undersöka och prediktera beteendet och motståndskraften hos några stålkvaliteter som används i överhettare och pannväggar i tungmetallrika förhållanden och höga materialtemperaturer. Omfattande laboratorie-, småskale- och fullskaletester utfördes. Resultaten kan direkt utnyttjas i praktiska applikationer, t.ex. vid materialval, eller vid utveckling av korrosionsmotverkande verktyg för att hitta initierande faktorer och förstå deras effekt på högtemperaturkorrosion.

Laboratoriestudien innefattar test där stålbitar utsattes för ren $ZnCl_2$, ZnO, $PbCl_2$ och PbO. Utöver dessa rena salter testades också saltblandningarna $ZnCl_2$-K_2SO_4, $PbCl_2$-K_2SO_4, $PbCl_2$-KCl och $PbCl_2$-$ZnCl_2$-KCl. Resultaten visar att ren $PbCl_2$ börjar bli aggressiv redan från 350 °C vilket är under smälttemperaturen (501 °C) på låglegerat stål (10CrMo9-10) och på rostfritt stål (AISI 347). Det skyddande Cr_2O_3-skiktet på det rostfria stålet förstördes pga. $PbCrO_4$-bildning. Då det låglegerade stålet utsattes för $ZnCl_2$ påvisades en ökad oxidskiktsbildning redan vid 350 °C, men endast en obetydlig oxidskiktsbildning på det rostfria stålet upp till 450 °C. Vid temperaturer över 350 °C minskade oxidskiktsbildningen pga. accelererad förångning av $ZnCl_2$.

Testen med $ZnCl_2$- och $PbCl_2$-blandningar ($ZnCl_2$-K_2SO_4, $PbCl_2$-K_2SO_4, $PbCl_2$-KCl och $PbCl_2$-$ZnCl_2$-KCl) visade att $PbCl_2$-$ZnCl_2$-KCl var mest aggressiv och reaktiv vid lägre temperaturer än de blandningar som innehöll $PbCl_2$-KCl. Därför antas $ZnCl_2$ har större tendens att förorsaka problem vid lägre materialtemperaturer, medan $PbCl_2$ förväntas vara problematisk vid de temperaturer som förekommer i pannans väggar och överhettare. Vid

400 °C uppmättes den högsta korrosionshastigheten på båda testmaterialen då både $PbCl_2$ och $ZnCl_2$ fanns i saltblandningen. $PbCl_2$-$ZnCl_2$-KCl-blandningen hade den högsta andelen smälta av alla testade blandningar, men uppvisade inte den högsta korrosiviteten vid alla temperaturer. Det här visar att korrosionshastigheten inte är direkt beroende av andelen smälta. Vid temperaturer över 500 °C orsakade alla tre $PbCl_2$-innehållande saltblandningar signifikant korrosion och båda stålkvaliteterna var lika skadade. Resultaten från experimenten med saltblandningar som innehöll 5 vikts-% $PbCl_2$ liknade resultaten från experimenten med ren $PbCl_2$. I bägge fallen hade salten orsakat extrem korrosion.

ZnO var varken korrosiv på det låglegerade stålet eller på det rostfria stålen vid 550 °C. Oxidskiktets tjocklek kunde väl jämföras med det skikt som åstadkommits utan något som helst salt. På 10CrMo9-10 förorsakade emellertid PbO ett märkbart oxidskikt vid 550 °C, och ett tunnare oxidskikt på AISI 347.

För att bättre förstå vad som händer med Zn samt dess roll i högtemperaturkorrosion, speciellt i returträeldade fluidbäddpannor, gjordes sondexperiment i en 30 kW_{th} bubblande fluidbäddpanna. I pannan brändes träpellets som dopats med $ZnCl_2$. Både beläggningar och korrosion undersöktes från sondringarna efter experimenten. Specifika frågeställningar i den här studien var de generella effekterna av höga halter Zn och Cl då man eldar returträ, samt utvärderingen av högtemperaturkorrosion förorsakad av $ZnCl_2$. Resultaten från experimenten visade att $ZnCl_2$ spelar en stor roll vid högtemperaturkorrosion av låglegerade stål. Då man jämför med motsvarande experiment då endast träpellets har eldats kan man konstatera att korrosion i fallet med $ZnCl_2$ redan förekommer vid 450 °C (den luftkylda sondens temperatur). K_2ZnCl_4 hittades i beläggningen och konstaterades vara den huvudsakliga korrosiva komponenten.

Under planeringen av fortsatta experiment stötte man på starka indikationer på att högtemperaturkorrosion av eldstadens väggar förorsakats av brom. Därför gjordes en mätkampanj i en bubblande fluidbäddpanna där SRF samförbrändes med träpellets. Både rökgaserna och beläggningarna analyserades för att undersöka förekomsten av korrosiva Cl-, Br-, Zn- och Pb-föreningar i bränslet. Kloridernas och bromidernas relativa korrosivitet studerades med hjälp av laboratorie-experiment. En $ZnBr_2$-K_2SO_4–saltblandning testades och jämfördes med motsvarande $ZnCl_2$-K_2SO_4-saltblandning. Blandningen med $ZnBr_2$ var mera aggressiv vid 400 °C under oxiderande förhållanden än motsvarande blandning med $ZnCl_2$. En mätkampanj visade att rökgasen i pannan var berikade med Cl tillsammans med små mängder Br, samt Zn och Pb. Termodynamiska jämviktberäkningar indikerade att möjliga föreningar på pannväggarna (400 °C) är Na- och K-bromider och -klorider, i oxiderande atmosfär samt dessutom Zn- och Pb-sulfider i reducerande atmosfär. Jämviktsberäkningarna korrelerade väl med resultaten från beläggningsanalyserna.

List of publications

This thesis is based on the work contained in the following papers:

I. Experimental Studies of Zn and Pb Induced High Temperature Corrosion of Two Commercial Boiler Steels.
D. Bankiewicz, S. Enestam, P. Yrjas, M. Hupa. **Fuel Processing Technology** (2012), doi:10.1016/j.fuproc.2011.12.017

II. High temperature corrosion of steam tube materials exposed to zinc salts.
D. Bankiewicz, P. Yrjas, M. Hupa. **Energy&Fuels**, 23 (2009) 3469-3474

III. Determination of the corrosivity of Pb-containing salt mixtures.
D. Bankiewicz, P. Yrjas, M. Hupa. **Submitted manuscript**

IV. Role of $ZnCl_2$ in High-Temperature Corrosion in a Bench-Scale Fluidized Bed Firing Simulated Waste Wood Pellets.
D. Bankiewicz, E. Alonso-Herranz, P. Yrjas, T. Laurén, H. Spliethoff, M. Hupa. **Energy&Fuels**, 25 (2011) 3476-3483

V. High temperature corrosion of boiler waterwalls induced by chlorides and bromides. Part 1: Occurrence of the corrosive ash forming elements in a fluidised bed boiler co-firing solid recovered fuel.
P. Vainikka, D. Bankiewicz, A. Frantsi, J. Silvennoinen, J. Hannula, P. Yrjas, M. Hupa. **Fuel**, 90 (2011) 2055-2063

VI. High temperature corrosion of boiler waterwalls induced by chlorides and bromides. Part 2: Lab-scale corrosion tests and thermodynamic equilibrium modeling.
D. Bankiewicz, P. Vainikka, D. Lindberg, A. Frantsi, J. Silvennoinen, P. Yrjas, M. Hupa. **Fuel**, 94 (2012) 240-250

Author's contribution

Paper I.

Bankiewicz, D planned the corrosion tests in collaboration with Enestam, S and other project partners. The experimental work was performed by Bankiewicz. The equilibrium calculations were performed by Enestam, S. The results from the laboratory experiments were evaluated by Bankiewicz, D and Enestam, S. Bankiewicz, D was the main writer of the paper.

Paper II.

Bankiewicz, D planned the corrosion tests in collaboration with co-authors of the paper. The laboratory tests and evaluation of the results was carried out by Bankiewicz, D who was the main writer of the paper.

Paper III.

Bankiewicz, D planned the corrosion tests, performed the laboratory experiments and evaluated the results. Bankiewicz, D was the main writer of the paper.

Paper IV.

Bankiewicz, D planned the bench-scale experiments together with other co-authors. The tests were carried out by Bankiewicz, D and Alonso-Herranz, E. The preparation of the samples and evaluation of the results were carried out mainly by Bankiewicz, D with help of Alonso-Herranz, E. Bankiewicz, D was the main writer of the paper.

Paper V.

Vainikka, P was the main author of the paper. He planned the experimental work, and performed part of it. Bankiewicz, D collected and prepared waterwall deposits samples, evaluated and reported SEM-EDX results.

Paper VI.

Bankiewicz, D planned the work in collaboration with Vainikka, P. The laboratory corrosion tests and the evaluation of the corrosion results were carried out by Bankiewicz, D, the equilibrium calculations were carried out by Lindberg, D. The interpretation of the thermodynamic equilibrium modelling results in connection to the vaporized ash-forming matter described in Part 1 was carried out by Vainikka, P together with Lindberg, D.

Related publications not included in the thesis:

VII. High temperature corrosion of steam tube materials exposed to zinc salts.
D. Bankiewicz, P. Yrjas, M. Hupa. **Impacts of Fuel Quality on Power Production and Environment** (2008) Banff, Canada. Conference Proceedings.

VIII. First results of deposit and corrosion tests using a high temperature corrosion probe in a 30 kW BFB during combustion of wood pellets doped with Zn.
D. Bankiewicz, E. Alonso-Herranz, P. Yrjas, T. Laurén, H. Spliethoff, M. Hupa. **Finnish- Swedish Flame Days** (2009) Naantali, Finland. Conference Proceedings

IX. High temperature corrosion of thermally sprayed NiCr- and amorphous Fe-based coatings covered with a KCl-K_2SO_4 salt mixture.
T. Varis, D. Bankiewicz, P. Yrjas, T. Suhonen, S. Tuurna, K. Ruusuvuori, S. Holmström, J. Salonen. **The 9th Liège Conference on Materials for Advanced Power Engineering** (2010) Liège, Belgium. Conference Proceedings.

X. Experimental studies of Zn and Pb induced high-temperature corrosion of two commercial boiler steels.
D. Bankiewicz, S. Enestam, P. Yrjas, M. Hupa. **Impacts of Fuel Quality on Power Production and the Environment** (2010) Saariselkä, Finland. Conference Proceedings.

XI. Laboratory High-temperature Corrosion Studies of Superheater Materials Exposed to KCl, $ZnCl_2$ and $PbCl_2$.
P. Yrjas, D. Bankiewicz, M. Hupa. **The 35th International Technical Conference on Clean Coal & Fuel Systems** (2011) Clearwater, Florida, USA. Conference Proceedings.

XII. Performance of superheater materials in simulated oxy-fuel combustion conditions.
D. Bankiewicz, S. Tuurna, P. Yrjas, P. Pohjanne. **EUROCORR 2011 – The European Corrosion Congress** (2011). Stockholm, Sweden. Conference Proceedings.

XIII. The corrosivity of alkali chlorides on superheater steels; Are KCl and NaCl equally corrosive?
S. Enestam, D. Bankiewicz, J. Tuiremo, K. Mäkelä, M. Hupa. **Fuel** (2012) In Press

List of abbreviations

RE Renewable energy

CHP Combined heat and power

EU European Union

WFD Waste Framework Directive

WtE Waste-to-energy

BFB Bubbling fluidized bed

SRF Solid recovered fuel

FB Fluidized-bed

CFB Circulating fluidized bed

RWW Recovered waste wood

MSW Municipal solid waste

CEWEP Confederation of European Waste-to-Energy Plants

CEN/TC European Committee for Standardization/Technical Committee

RDF Refuse derived fuel

PVC Polivinylchloride

BFRs Brominated flame retardants

mpy milli inch per year, 1 mpy=0.025 mm/y

NTP Normal temperature and pressure

SEM/EDX Scanning electron microscope/energy dispersive x-ray

BSE Backscattered electrons

SE Secondary electrons

CL Cathodoluminescence

DLPI Dekati-type Low Pressure Impactor

ELPI Electric Low Pressure Impactor

GC Gas chromatograph

FTIR Fourier Transform Infra-Red

IC Ion chromatograph

ICP-MS Inductively coupled plasma mass spectrometry

$\mathbf{T_m}$ Melting temperature

XRD X-ray diffraction

RBU Rate of deposit buildup

Table of contents

Preface i
Abstract iii
Svensk sammanfattning v
List of publications vii
Author's contribution viii
List of abbreviations x
Table of contents xii
1. INTRODUCTION 1
1.1 Objectives 2
1.2 Approach 3
2. BACKGROUND 3
2.1 Fluidized Bed technology 3
2.1.1 Bubbling Fluidized Bed boiler 4
2.2 Selection of boiler tube materials 6
2.3 Waste fuels containing Zn and Pb 8
2.3.1 Recovered waste wood (RWW) 8
2.3.2 Municipal solid waste (MSW) 9
2.3.3 Solid recovered fuel (SRF) 9
2.3.4 Refuse derived fuel (RDF) 9
2.4. Sources of Zn, Pb, Cl and Br in waste fuels 10
2.5 Corrosion in waste fuel fired boilers 11
2.5.1 (Alkali) Cl-induced corrosion 12
2.5.2. Speciation of Zn and Pb during combustion of waste-derived fuels 13
2.5.3 Corrosion by Zn and Pb containing deposits 14
2.6 Concluding remarks on the literature 17
3. EXPERIMENTAL METHODS 18
3.1 Laboratory method for high-temperature corrosion tests 18
3.1.1 SEM-EDX 21
3.2 Bench-scale measurements 21
3.2.1 Bench-scale BFB reactor 21
3.3 Full-scale measurements 23
3.3.1 BFB boiler 23

3.3.2 Waterwall deposit sampling 23
3.3.3 Aerosol sampling 24
3.3.3.1 IC and ICP-MS (DLPI) 25
3.3.4 Thermodynamic modelling procedure 25
4. RESULTS AND DISCUSSION *27*
4.1 Corrosion laboratory tests with Zn- and Pb-containing synthetic deposits 27
4.1.1 Tests with single salts; $ZnCl_2$, $PbCl_2$, ZnO and PbO 27
4.1.2 $ZnCl_2$ and $PbCl_2$ containing mixtures 30
4.1.3 $ZnCl_2$-K_2SO_4 and $ZnBr_2$-K_2SO_4 34
4.2 Corrosion during firing of wood pellets doped with $ZnCl_2$ 37
4.3 Waterwall corrosion & determination of the corrosive species during co-firing of SRF . 39
4.3.1 Vapours and gas composition 39
4.3.2 Deposits 40
4.3.3 Thermodynamic equilibrium calculations 42
5. CONCLUSIONS *43*
REFERENCES *46*

1. INTRODUCTION

The utilization of waste materials through combustion and co-combustion increases their contribution to the energy requirements of many countries. With rising fossil fuel prices, the attractiveness of waste fuels increases. Waste fuels are abundant and cost-competitive energy sources. Renewable Energy (RE) from waste is claimed to be a much cheaper source of Renewable Energy than from most other RE sources (solar, wind, biomass) [1]. The steam generated from waste combustion or co-combustion is utilized either for electricity production or for district heating or for both in combined heat and power plants (CHP). Combustion/co-combustion of waste and waste-derived fuels has other significant advantages apart from energy recovery. It diverts material from landfills and avoids disposal costs, it reduces CO_2 emissions via replacement of fossil fuels, it reduces the emissions of methane coming from landfills and it has low environmental impact thereby conforming to strict directives [2, 3].

Until 2000, there was no legal ruling in the European Union (EU) obliging the recovery of energy from the incineration or co-incineration process. In December 2000, the Directive 2000/76/EC [4] on the incineration of waste came into force. It stated that "any heat generated by the incineration or the co-incineration process shall be recovered as far as practicable." The new Waste Framework Directive 2008/98/EC (WFD) [5] which came into force on 12 December 2008 allows highly efficient Waste to Energy Plants (WtE) to be classified as energy recovery facilities rather than waste disposal, provides an important impetus for the WtE plants to acquire "energy recovery status". To reach this status, however, a certain energy efficiency factor needs to be achieved, requiring that WtE plants need to improve their energy performance. The new Directives, that stipulate that the target of 20% renewable energy set by EU in Directive 2009/28/EC [6] is reached, require an increase in power production efficiency in steam boilers as well as in WtE plants. This requirement has brought the challenges of optimizing the waste combustion process. One alternative to increase the electricity (and heat) production efficiency is to increase the steam parameters. The rise of steam temperature and pressure especially in waste-fired boilers significantly increases the risk of fireside corrosion and thus exposes plants to unplanned shut-downs and costly replacements of heat exchanger. A full bundle of superheaters for a 100 MW combined heat and power boiler has been estimated to easily exceed the cost of 1 MEuro [7]. Many power plants that burn challenging fuels experience failures of the boiler superheaters and/or increased waterwall corrosion due to aggressive fuel components (already at low temperatures). Therefore, in order to minimize problems in metal tube corrosion in waste-fired boilers, the steam temperature is currently kept at a relatively low level. This factor, however, limits power production efficiency to roughly 25% and such performance is not satisfactory from the profitability point of view of the plant [8, 9].

The elements found in waste and waste-derived fuels that are commonly associated with high-temperature corrosion are: chlorine (Cl), sulfur (S), there are also indications of bromine (Br); alkali metals, mainly potassium (K) and sodium (Na) and heavy metals such as lead (Pb) and (Zn). The two last may be present in the fuels at concentrations exceeding 1 wt-%, which may result in significant amounts of heavy metals in the deposits [9-17].

Upon combustion, Zn and Pb may react with S and Cl to form chlorides and sulphates in the flue gases [18]. These specific heavy metal compounds are of special concern due to the formation of low melting salt mixtures. Low-melting compounds entrained in the flue gases pass the convective parts of the boiler and may stick to colder surfaces of furnace walls and superheaters forming aggressive deposit that increases the risk of corrosion (additionally) enhanced by the presence of molten salts [17, 19].

In waste-fired boilers the waterwall steel temperatures typically range from 300 °C to 400 °C [20]. Alkali chloride (KCl, NaCl) induced high-temperature corrosion has not been reported to be particularly relevant at such low material temperatures but rather at temperatures close to 500 °C and higher [21]. However, the presence of Zn and Pb chlorides in the deposits that leads to the formation of low temperature melts has been found to induce corrosion already in the 300-400 °C temperature range [20, 22-24].

In order to predict the behaviour and resistance of boiler superheater and waterwall materials during the combustion of demanding fuels, including at increased steam parameters, it is of considerable importance that there should be extensive research on that subject. The boiler owners tend to move towards increasingly complicated fuels and fuel mixtures. This is also a big challenge for the boiler manufacturers and since it is difficult and sometimes expensive to make full-scale corrosion tests over longer periods of time, it also provides a motive to develop and perform corrosion tests in both the laboratory and in small-scale units where testing of different boiler steels in simulated combustion atmospheres is carried out. The laboratory tests give indications in a relatively short time about the corrosiveness of the tested conditions, and they are relatively inexpensive. The results can usually be used in practice, for example in the initial selection of the materials. The results of the laboratory tests help to find triggers initiating corrosion, and they help in understanding the role of certain elements and their effect on high-temperature corrosion, and that often results in the development of preventive tools.

The temperature range of waterwall and superheater materials in biomass and waste fired boilers is typically between 260-540 °C. In this thesis, the term high-temperature corrosion refers to corrosion in the 250-600 °C temperature range.

1.1 Objectives

This work focuses on high-temperature corrosion of boiler tube materials induced by Zn and Pb. The available literature deals to some extent with Zn related corrosion problems, but very little attention has been paid to the role of Pb compounds. The mechanisms of high-temperature corrosion in the Zn and Pb rich environments are not yet fully understood. The objective of this work was to get better insight into high-temperature corrosion induced by Zn and Pb, to estimate the relative corrosiveness of Zn and Pb containing compounds as a function of temperature, and to try to establish mechanisms by which metal wastage in environments containing these heavy metal compounds occur.

1.2 Approach

This thesis consists of six papers in which experimental work and measurements related to high-temperature corrosion were carried out in laboratory, bench-scale and full-scale tests. Firstly, pure $ZnCl_2$, ZnO, $PbCl_2$ and PbO were tested on low-alloy and stainless steel to study the difference in the corrosiveness of Zn and Pb chlorides and oxides as a function of temperature (**Paper I**). As a continuation of the research, further laboratory tests with salt mixtures containing $ZnCl_2$ and $PbCl_2$ were carried out (**Papers II & III**). To better understand the fate of Zn and its role and effect on high-temperature corrosion specifically in waste-wood fired fluidized bed boilers, high-temperature corrosion/deposit probe tests were performed in a 30 kW_{th} bubbling fluidized-bed (BFB) reactor firing wood pellets doped with $ZnCl_2$ to simulate waste wood. Specific issues of interest in this study included the general impact of firing waste wood containing higher amounts of Zn and Cl and evaluation of the role of $ZnCl_2$ in high-temperature corrosion (**Paper IV**). During the planning stage of further experiments there were strong indications of bromides induced high-temperature corrosion of the waterwalls. In consequence, a measurement campaign in a BFB co-combusting solid recovered fuel (SRF) was performed to determine the occurrence of corrosive Cl-, Br-, Zn- and Pb-compounds in the fuel, in the furnace vapours and in the waterwall deposits. Since both Cl and Br were found in the corrosion front, the second part of the work was focused on determining the relative corrosiveness of chlorides and bromides by means of laboratory experiments. $ZnBr_2$-K_2SO_4 containing salt mixtures were chosen for testing because further comparison with corresponding $ZnCl_2$ containing mixtures used in previous tests was then possible (**Papers V & VI**).

2. BACKGROUND

The most common technologies for heat and electricity production from waste are nowadays incineration in grate fired boilers in WtE plants and in fluidized-bed boilers [25]. The following chapter gives a brief description of fluidized-bed (FB) technology and emphasizes the bubbling fluidized-bed type since this type of boiler was used in two experimental studies performed in this work. Further, BFBs boilers are more commonly used when biomass, or other highly reactive, low-grade fuels are used [26]. The chapter also describes typical groups of commercially available boiler tube materials used in power plants, focusing on the materials that were selected for testing in this work. This part gives also an overview of the waste fuels rich in Zn and Pb. The chapter contains also a thorough literature review on available research concerning Zn and Pb related corrosion problems in industrial boilers.

2.1 Fluidized Bed technology

The studies on fluidized-bed technology for power generation evolved at the end of 50's and the beginning of the 60's, when research on coal combustion in fluidized-beds was initiated by the British Coal Utilization Research Association and the National Coal Board of the UK. The idea of burning coal in FB instead of gasifying was promoted by Douglas Elliot from the early 60's [27]. At the beginning of the 80's it was affirmed that the development of FB

boilers had reached the commercial phase for both heat and electrical energy production [28, 29].

A fluidized-bed boiler is a type of steam generator where fuel is burnt in a fluidized state. The fluidized bed is based on the even distribution of air or gas upward through fine bed material e.g. sand. The fuel constitutes only a minor fraction of the total bed material (1-3%). The bed is said to be *fluidized* when the individual particles are suspended in the air stream.

There are two principal types of fluidized bed boilers:

- Bubbling fluidized bed (BFB) - with increase in air velocity the bed of solid particles behaves like a boiling liquid – it fluidizes.
- Circulating fluidized bed (CFB) - at higher air velocities than in the BFB bubbles disappear and the bed particles fill the whole freeboard and are recirculated via cyclones to the bed.

Both types can be designed to operate under either atmospheric pressure (for steam generation) or under high pressure (in combined-cycle applications).

2.1.1 Bubbling Fluidized Bed boiler

Bubbling fluidized bed boilers are quite common for the combustion of fuels characterized by low heating value, high moisture, high volatiles and low char content such as biofuels, and for low grade fuels such as (waste) recycled fuels. CFB boilers are mainly used for combustion of coals [26, 28]. The fuel flexibility in BFB boilers is possible since the combustion temperature is kept at a relatively low level, about 800-900 °C, thereby reducing risk of fouling and slagging. The possibility of combustion or co-combustion of diverse fuels is one of the biggest advantages of BFB boilers. Typical parameters of BFB units [25, 28] are:

a) capacity

- 1-50 MW_{th}, but there are also larger units with installed capacity up to 300 MW_{th}

b) working fluid

- water in the economizers 130-350 °C
- water in the furnace walls 250-350 °C
- saturated/superheated steam up to 170 bar/540 °C (the surface temperatures of superheaters are usually 35-50 °C higher than the steam temperature in the tubes)

c) steam capacity

- 2-160 t/h and more

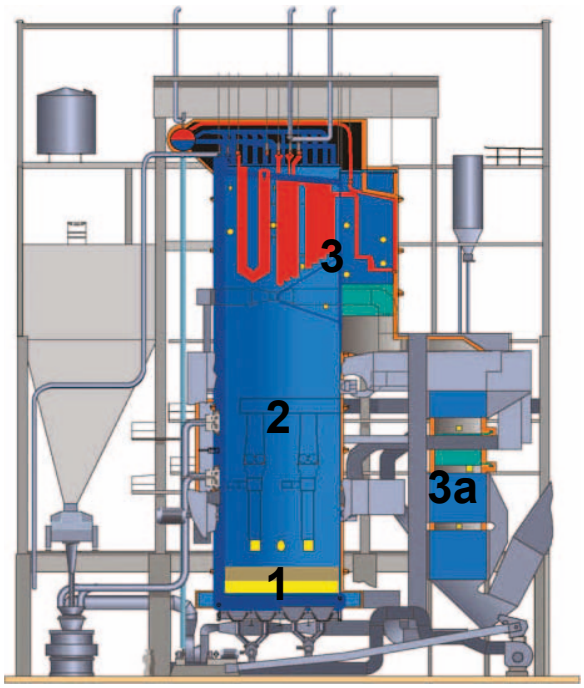

Figure 1. Schematic picture of Stora Enso Anjalankoski co-incinerating BFB boiler [10]. 1. Lower furnace, 2. Freeboard, 3. Convective section (tertiary, secondary and primary superheaters), 3a. Convective section (economizers and air preheaters).

A typical bubbling fluidized-bed boiler is shown in Figure 1. This specific boiler is described in more detail in *Section 3.3.1.* A BFB boiler can be divided into three major sections:

1. *Lower furnace* – the bottom of the furnace is composed of a grate with nozzles through which primary combustion air is distributed into the fluidizing bed, which commonly consists of sand and ash. The fuel can be fed into the boiler, depending on the fuel, in two ways: over-bed or below the bed surface. The fuel constitutes only a small fraction of the bed material, around 1-3% and its combustion takes place mostly in the bed. The walls of the lower furnace hold the bed material and are made of refractory material which minimizes heat loss from the bed and protects waterwalls from erosion.

2. *Freeboard* – is the space above the bed. In this section there are the secondary and tertiary air ports. In the freeboard combustion of the finer particles and volatiles continues. The furnace walls are usually composed of tubes forming membrane waterwalls. The water enters the waterwall tubes at the bottom of the furnace and the heat from the combustion turns it into a water/steam mixture which rises due to the density difference and leaves the waterwall tubes at the top and enters the steam drum.

3. *Convective section* – steam from the steam drum is directed to the superheaters which are part of the convective section where steam is superheated above the steam

saturation point. Typically, a BFB consists of primary, secondary and tertiary superheaters. Out of all parts of the boiler's convective section, the tertiary and secondary superheaters are the hottest, so the most susceptible to corrosion. Economizers and air preheaters are placed further in the flue gas duct where the flue gases and material temperatures are much lower but the conditions, though less harmful, are often still corrosive [25, 29].

2.2 Selection of boiler tube materials

To ensure efficient and economical performance and availability of the boiler proper materials for the superheaters, preheaters and membrane waterwalls must be selected. The desired mechanical and physical properties of materials for boiler heat transfer surfaces are predominantly: corrosion resistance (also resistance to steam-side oxidation); yield strength (part of the boiler tubes is in the temperature range where yield strength is crucial and is used as the dominating design criterion); creep rupture strength (the stress which, at a given temperature and in a given time will cause a material to rupture); ductility (determining the suitability of a material for a given application); and weldability (ability of the materials to be welded). Important aspects in selecting materials suitable to the particular application include the information of the target, maximum operation temperature (this affects also tube wall temperature), flue gas temperature and composition, local atmosphere, and fuel composition. Beside the mechanical requirements, the price of the materials also plays an important role, so the selection of boiler tube materials starts from the cheapest carbon steel, moving to low-alloy steels, to high-alloy steels, and then to the most expensive stainless steel/austenitic stainless steels etc. to meet the critical demands of the combustion environment [30, 78]. The costs of superheater materials are large and the length of the steel tubes needed for the manufacture of heat transfer parts can be counted in kilometers. As indicated by Enestam [25] the cost of one tertiary superheater for a large-scale BFB can vary between 100,000 and 500,000 € depending on whether a low-alloy or a high chromium steel is chosen.

The materials chosen for testing in this work were selected to represent different the groups of the steels: non-alloy steel (St.45.8/III), low-alloy steel (10CrMo-9-10), and austenitic stainless steels (AISI 347 and Sanicro 28). Those steel groups are briefly described in this section.

The most interesting materials based on resistance and costs are non-alloy (carbon steel) and low-alloy steels to which very little of alloying elements are added. Carbon steel is made of iron and carbon, the latter responsible for steel's properties. Low carbon content (<0.2%) influences the elasticity of iron. With increasing carbon content (up to 1%) the steel becomes harder and stronger but more difficult to weld [31]. The low-alloy steels are alloys of iron and <5% of other alloying elements such as Cr, C, Mn, Mo, Si and P. The minor alloying elements have the role of improving steel's mechanical properties and resistance to corrosion/oxidation. Some of the elements that improve steel's properties may even, in certain corrosion environments, have a harmful effect on the corrosion resistance [32]. For example Mo increases oxidation resistance but alloys containing 3-4% Mo are basically designed to withstand reducing, acid conditions and are not well suited for oxidizing conditions [33]. On the other hand Mn improves weldability and increases the strength of metal, but is not a

desired element when resistance against sulfidation is required [34]. Thus when choosing an application for a material its composition, including minor alloying elements, must be well studied. The low-alloy materials are popular due to their low cost, versatile properties, and wide range of available grades. The maximum temperature range allowed for the use of low-alloy steels (depending on alloying elements) is estimated to be 500-570 °C [78]. However, low-alloy steels may not always provide the desirable resistance against high-temperature corrosion, especially in aggressive environments. So, in order to withstand more demanding environments and elevated temperatures steels with higher Cr content are the next choice. The Fe-Cr steels with 5-12.5% Cr are called high-alloy steels while the iron-based steels with more than 13% Cr, 0-22% Ni and minor amounts of C, Nb, Cu, Mo, Se, Ta, and Ti are in general called stainless steels. These materials have high corrosion and heat resistance and are easily fabricated. The corrosion resistance of stainless steels relies on passive Cr_2O_3 layer formation which provides protection from further oxidation of the metal. The increasing Cr content improves corrosion resistance in more severe environments, including at elevated temperatures. Fluctuating temperatures, however, cause the expansion of metal/oxide leading to spalling and/or cracking of the protective scale, exposing unprotected metal to further oxidation. In the absence of oxygen the formation of protective oxide is retarded and metal is exposed to direct attack. The stainless steels can be divided according to their metallurgical structure (for example): ferritic (with a body-centred cubic crystallographic structure), martensitic (distorted tetragonal structure), austenitic (face-centred cubic structure) and duplex (containing roughly 50% of austenite and 50% of ferrite). Pure iron has a body-centred crystallographic structure (ferrite). However, when certain elements (also called austenite formers) are added to stainless steel, notably Ni but also C, N, Mn and Co, the structure changes from body-centered to face-centered and austenite is formed. These small changes noticeably influence the properties of the steel, and therefore the austenitic stainless steels have the widest usage of all stainless steels due to their beneficial corrosion resistance, good mechanical properties and ease of fabrication. To achieve benefits in the form of increased resistance to corrosion, the austenitic stainless steels usually contain more Cr. But to induce the transition from ferritic to austenitic, the addition of Ni is required along with increasing Cr content in the steel. The price of Ni significantly exceeds that of Cr, so the relative price of austenitic stainless steels can be as much as 25 times higher than the price of low-alloy steels (as indicated in Table 1) [25, 35]. Many alloys demonstrate excellent corrosion resistance but those materials may have poor strength at high temperature and pressure that significantly limits the utilisation of such alloys. Composite tubes consist of two different materials which are metallurgically bonded together. An internal layer, which is composed of non-alloy or low-alloyed steel is clad with a highly alloyed stainless steel or nickel based material. Cladding not only improves the corrosion resistance but also adds strength to the tube [36, 78].

The detailed composition of common boiler tube materials, which were exposed to high-temperature corrosion tests and further investigation within this work are listed in Table 1.

Table 1. Common boiler tube materials tested within this work.

Name	Category	Relative price/kg[a]	Application	Elements, wt-%[d]								
				Fe	Cr	Ni	C	Mo	Mn	Si	Nb	P, S
St.45.8/III	Non-alloy steel	1.5	membrane walls	95,8	0,2	-	2,85	-	0.8	0.3	-	<0.2
10CrMo9-10	Low-alloy steel	3	superheaters[c]	95,9	2,2	-	0,07	1.0	0.4	0.2	-	<0.2
AISI 347	Austenitic stainless steel	8.5	superheaters[c]	68,7	18,1	10,9	0,04	-	0.9	0.5	0.8	<0.2
Sanicro 28	High-alloy austenitic stainless steel	28[b]	superheaters	36,1	27,4	31,9	0,11	3.5	1.1	0.5	-	<0.2

[a] March 2012, [b] price for composite tube, [c] taken from Enestam, S [25], [d] analysed with SEM

2.3 Waste fuels containing Zn and Pb

Since Zn and Pb have been found in considerable amounts in deposits in waste-fired boilers [20, 37] some waste-fuels that contain these elements are presented in this chapter.

2.3.1 Recovered waste wood (RWW)

Recovered waste wood (RWW) includes all kinds of wood material that is available at the end of its use as a wood product and originates mainly from construction and demolition activities and from commercial and industrial sources. However, it usually also contains non-wood components such as metal parts (nails, handles, screws, hinges, wires, fittings), plastics (flooring, wallboards, sheeting, electrical wires), paints and surface treatments (siccatives, binders, preservatives) [38]. The price of RWW makes it a more attractive fuel compared to pure wood. As indicated by the Swedish Energy Agency, the prices of RWW during the last few years were 40-60% lower than those of various types of virgin wood [39]. Krook et al. [40] published the average amounts of the contaminating materials present in RWW:

- Surface-treated wood 15 wt-%
- Preservative-treated wood 3.5 wt-%
- Soil 0.6 wt-%
- Plastics 0.1 wt-%
- Iron/steel 0.5 wt-%
- Concrete 0.05 wt-%

An estimation of the amount of waste wood in 20 of the 22 European Union (EU) member countries (Austria, Belgium, Bulgaria, Croatia, Denmark, Finland, Germany, Greece, Hungary, Ireland, Italy, Netherlands, Norway, Poland, Portugal, Romania, Serbia, Slovenia, Spain, Sweden, and U.K.) showed that about 30 million tons are produced annually, which corresponds to about 13% of the annual round wood consumption of 227 million tons and about 444 PJ/a or 0.7% of the total energy consumption of 67 000 PJ/a. Another source says that around 10 million tons of waste wood is produced yearly only in the U.K., most of which goes to landfills [38]. Currently within the EU 34% of waste wood is used for power generation, 38% is being recycled; and 28% is being composted or put into landfills [41].

2.3.2 Municipal solid waste (MSW)

MSW is a heterogeneous fuel with no or little pre-processing originating from domestic and industrial sources. Vainikka [42] compiled MSW composition data from different sources and the main MSW fractions are as follow:

- Organics 30-40 wt-%
- Paper/Cardboard 15-25 wt-%
- Plastics 7-15 wt-%
- Metal, glass, textiles 1-7 wt-% (each)
- Other 18-30 wt-%

According to the Confederation of European Waste-to-Energy Plants (CEWEP), which covers 90% of the Waste-to-Energy Plants in Europe about 69 million tonnes of household and similar waste that remains after waste prevention, reuse and recycling, was treated in WtE plants in Europe in 2008. That is equivalent to 28 billion kWh of electricity and 69 billion kWh of heat [43]. Overall incineration in EU-27 (with or without energy recovery) accounted for 129 million tonnes of treated MSW in 2008. The amount of incinerated MSW and similar waste has increased by 20% since 2004. The described growth results from continuously increasing incineration of MSW and refuse-derived fuels for power production [44].

2.3.3 Solid recovered fuel (SRF)

Solid recovered fuels (SRF) has to be distinguished from other waste-derived fuels, often called refuse derived fuels (RDF), which do not meet the requirements of the European CEN-TC standard. SRF is a fuel derived from MSW and commercial & industrial waste through industrial processes and can be considered as waste-derived fuel, the quality of which is controlled, classified and certified according to the European Committee for Standardization – CEN/TC 343 [45]. SRF contains mainly:

- Paper 40-50 wt-%
- Plastics 25-35 wt-%
- Textiles 10-14 wt-%

High amount of plastics contributes to high calorific value of the fuels, thus SRF's derived from MSW have lower heating value than when derived from selected commercial waste [46, 47]. SRF is divided into 5 classes which are determined by boundary values of specific fuel properties which are relevant to economic factors (heating value), technological restrictions (amount of Cl) and environmental aspects (Hg) [46].

2.3.4 Refuse derived fuel (RDF)

There is no standard definition of the term *Refuse Derived Fuel* and the term is interpreted differently in different countries [48]. Generally speaking RDF is a processed, high calorific fraction of MSW, meaning that the waste is shredded, sorted and fractions such as for example metals and glass are separated. The separation process increases the organic material,

thereby also increasing the heating value [70]. Below is an example of the major components in RDF produced in Attica/Greece [49].

- Printed paper 38 wt-%
- Packaging plastics 26 wt-%
- Packaging paper 16 wt-%
- Cloth 11 wt-%
- Other paper 5 wt-%
- Other plastics 1 wt-%
- Organics 1 wt-%
- Wood 0.5 wt-%

Although RDF has a similar composition as SRF, RDF does not meet CEN/TC 343 standards [45].

The production of RDF from MSW grows fastest in EU member countries i.e. Austria, Germany, Netherlands, with high levels of MSW source separation and recycling as the recycling generates high calorific residues suitable for RDF. The total quantities of RDF produced from MSW in the EU in 2003 have been estimated to amount to over 3 million tons and are increasing [48].

2.4. Sources of Zn, Pb, Cl and Br in waste fuels

Zinc

Galvanizing is one of the largest industrial applications of Zn [50]. Galvanized fastening systems are considered as a potential source of heavy metals, particularly of Zn. Another common source of Zn in waste fractions is brass (Cu-Zn alloy) as well as other alloys. Tinted glassware, apart from Si and Cu, also contains Zn [51]. Zn is also used in plastics as an acid scavenger and filler in the form of ZnO [52]. In recovered waste wood mainly surface treatments, such as white pigment in paints, contribute to an increase in the amounts of Zn [40, 53]. Zn is also a plant nutrient and is naturally present in small amounts in wood [54]. Moreover Pb- and Zn-containing compounds are widely used in PVC as stabilizers [55].

Lead

Nakamura et al. [56] found that up to 90% of the Pb in waste originates from batteries, glassware and electric appliances and light bulbs etc. If the highly contaminating items (batteries, glass, light bulbs) are excluded from waste the main sources of Pb are most likely to be plastics, textiles, rubber and leather, present as lead oxide (white pigment) and lead stearate [56]. Also, as mentioned already above, Pb is a common metal stabiliser used in PVC [52]. In RWW, Pb typically originates from different surface treatments such as siccatives and colouring pigments [40, 53].

Chlorine

It is generally known that the Cl present in waste originates mainly from chlorinated plastics, mainly polyvinylchloride (PVC), or food residues which contain dietary salt. Approximately 70% of the Cl in MSW has been estimated to originate from plastics, particularly PVC [48, 57]. In addition to its use in PVC, chlorine is used in flame retardants [58]. Wood surface treatments also contribute to increased levels of Cl. Those treatments may be paints and its additives, adhesives, binders etc. [59]. Cl is also a plant micronutrient and is present naturally in wood [60], so Cl present in RWW may originate to some extent from wood itself.

Bromine

Vainikka P., [42] compiled the major sources of bromine in solid waste fuels. It was reported that bromine is widely used in brominated flame retardants (BFRs) and over 90% of all electrical and electronic equipment is flame retarded. The SRF which is a fraction of MSW typically comprises 35–50% textiles and plastics [47, 61]. In both of these fractions flame retardancy is often required. Other important sources of Br resulting from the usage of BFRs but present to a smaller extent in solid waste fuels are building and construction applications in which construction board and extruded foams are utilize. Further, plastic parts used in the transportation sector may be mentioned [42]. Therefore, the likely sources of bromine in solid wastes are brominated flame retardants (BFRs) [62].

2.5 Corrosion in waste fuel fired boilers

In ambient atmosphere and temperature corrosion rates are determined by two essential factors: water and oxygen. At this temperature stainless steel will not corrode in dry or low humidity air, while an increasing temperature speeds up electrochemical and chemical reactions and that significantly increases corrosion rates. High-temperature environments such as the ones present in energy conversion systems where different fuels are burnt are complex. The atmosphere, apart from the effects of elevated temperatures, may be oxidising or reducing, containing gaseous, solid, semi-molten or molten, corrosive chemical compounds. Thus the overall nature of such environments is determined by the amounts of specific gases, vapours and molten chemical compounds [35].

High-temperature corrosion of superheaters in biomass boilers is frequently experienced and was assumed to be induced to a considerable extent by alkali (Na, K) chlorides [77]. There are hardly any reported waterwall corrosion experiences from the combustion of virgin biomass (wood, crops or their residues). With the introduction of, for example, recovered waste wood into biomass combustion, problems relating to deposit formation, aggravated superheater corrosion and corrosion of waterwalls have been reported [63-66]. Similar observations have been reported regarding municipal solid waste incineration as summarised by Wright and Krause [67], and the combustion of solid recovered fuel [10]. In the case of waste-fired boilers it was concluded that the NaCl and/or KCl and HCl which are present in high amounts could not have been the only cause of increased corrosion at lower (when comparing to biomass-fired boilers) material temperatures [68]. The problem of a corrosive environment in waste-fired facilities was already known in the mid-60's but then it was believed to occur

mainly due to reducing conditions [71]. Further investigations from the 70's and 80's showed that in the deposits from such facilities, in addition to the typically found elements (Na, K, S, Cl), elevated amounts of Zn and Pb were often identified. The problem of Zn and Pb rich corrosive deposits was then determined and investigated and still persists to this day [7, 17, 20, 22, 69-74]. Lately, indications of bromides induced high-temperature corrosion have also been reported [10].

2.5.1 (Alkali) Cl-induced corrosion

The available literature quite extensively covers problems of chloride related corrosion occurring mainly but not exclusively in biofuel fired boilers [75-79]. The chlorine/chlorides are described in literature to induce corrosion of superheaters in many ways. Generally it is accepted that it is either due to the flue gases containing Cl_2 and HCl which may cause direct corrosion or via deposition of alkali chlorides (NaCl, KCl) on superheater tubes. It was also suggested that the Cl-containing species may interact with SO_2 and/or SO_3 forming sulphates and enhancing corrosion by released Cl [80]. All those phenomena may be present and act together resulting in a greater corrosion than would result from gases or deposit alone [77, 80].

In oxidising conditions a dense oxide layer grows on the metal surface which provides protection from further oxidation and against other gaseous species. The high Cr steels rely on a formation of a dense and protective Cr_2O_3 layer, while iron oxides formed on iron-based steels are porous, thus providing only limited protection. The accelerated corrosion of metals due to the activity of the gaseous species Cl_2/HCl was first described by McNallan [81] and this phenomenon is often referred to as active oxidation. The active oxidation causes a linear oxide layer growth producing a non-protective oxide layer. Grabke et al. [79] presented this phenomenon later on by means of chemical reactions which are described further in the text. In order for active oxidation to occur, Cl_2 or HCl must be present in the flue gas/deposit which, if present, penetrates the oxide scale (present on each metal in an oxidizing environment) through the pores and cracks down to the metal surface and the metal chlorides (M=Fe, Cr, Ni) are formed according to reactions (1) and (2):

$$Me(s) + Cl_2(g) = MeCl_2(s,g) \quad (1)$$

$$Me(s) + 2HCl(g) = MeCl_2(s,g) + H_2(g) \quad (2)$$

The formed metal chlorides evaporate continuously due to their significant vapour pressure and diffuse outward (reaction (3)). Finally, in regions of higher oxygen partial pressure conversion into oxides takes place, reactions (4) and (5) [78]:

$$MeCl_2(s) = MeCl_2(g) \quad (3)$$

$$3MeCl_2(g) + 2O_2(g) = Me_3O_4(s) + 3Cl_2(g) \quad (4)$$

$$2MeCl_2(g) + 3/2\ O_2(g) = Me_2O_3(s) + 2Cl_2(g) \quad (5)$$

Salmenoja et al. [82] showed that in oxidizing conditions HCl enhances degradation of Fe and binary Fe-Cr steels but significant corrosion on high Cr alloys is observed only above 600 °C.

In combustion conditions HCl is the dominant gaseous Cl species. Wright and Krause [67] reported, however, that some elemental Cl_2 may possibly be formed in combustion products by oxidation of HCl. The metal oxide is serving as a catalyst and the formation of Cl_2 should be enhanced at low $p(H_2O)$ in the flue gases (Deacon Process), reaction (6). Hupa et al. [85] indicated additionally that reaction (6) at higher temperatures with increased H_2O and low O_2 favours the formation of HCl. Therefore, according to Hupa et al. [85] the corrosion induced by the presence of Cl_2 may be omitted in the lower furnace region in refuse-fired boilers, due to the high flue gas temperatures (exceeding 600 °C):

$$2HCl(g) + ½\ O_2(g) = Cl_2(g) + H_2O(g) \quad (6)$$

Alkali chlorides carried by flue gases may stick on the surface of boiler tubes forming corrosive deposits. The interaction of alkali chlorides with steels leads to the formation of non-protective chromates and ferrites and also to the release of Cl_2/HCl through interactions with the oxide scale [17, 78, 79, 83], e.g. reactions (7)-(9):

$$2(Na, K)Cl(s) + Fe_2O_3(s) + ½\ O_2(g) = (Na, K)_2Fe_2O_4(s) + Cl_2(g) \quad (7)$$

$$4(Na, K)Cl(s) + Cr_2O_3(s) + 5/2\ O_2(g) = 2(Na, K)_2CrO_4(s) + 2Cl_2(g) \quad (8)$$

or

$$4(Na, K)Cl(s) + Cr_2O_3(s) + 2H_2O(g) + 3/2O_2(g) = 2(Na, K)_2CrO_4(s) + 4HCl(g) \quad (9)$$

The Cl_2 released via reactions (4)-(8) is expected to be released mainly into the atmosphere, but Grabke et al. [79] reported that part of the Cl_2 may diffuse back to the metal/oxide interphase, repeating the chain of the described reactions, and as a result creating a cycle. The penetration of Cl_2 through the pores and cracks of the oxide scale as well as its cycle is not fully understood. According to Petterson et al. [84] and Lehmusto et al. [111] the significance of reactions (8) and (9) in the corrosion of stainless steels lies not only in the release of the Cl_2/HCl but also in the destruction of protective Cr_2O_3 by formation of alkali chromates, which is the mechanisms that initiates rapid corrosion at high temperatures.

In reducing conditions, the protective oxides do not develop or are discontinuous. The Cl-species can then react directly with the metal surface to form metal chlorides and the corrosion rates were shown to be higher in reducing than in oxidizing conditions [85].

2.5.2. Speciation of Zn and Pb during combustion of waste-derived fuels

Combustion of waste fuels in BFBs may cause that the flue gases will be enriched with zinc and lead compounds [86]. The Zn and Pb are found mostly in the form of oxides and salt of chlorine and sulfur in the ash but the dominating forms of those elements change continuously due to fluctuations in gas composition, temperature and ash composition [80]. There are also significant differences in the behaviour and volatility of Zn and Pb in reducing and oxidizing conditions [86]. The atmosphere in boilers firing waste-derived fuels is usually rich in HCl that promotes the formation of $ZnCl_2$, in addition to the more stable ZnO and $PbCl_2$. The Zn and Pb chlorides are mostly present in low-temperature zones, and are

characterised by higher volatility at higher temperature [87]. However the eutectic mixtures containing $ZnCl_2$ form a melt at waterwall temperatures, while mixtures with $PbCl_2$ (with some exceptions) are most likely to form melt at superheater temperatures [67]. When the conditions are reducing, both elements will be present as monoatomic gases. According to Backman et al. [86], formation of gaseous chlorides of Zn and Pb will be suppressed when alkalis (K, Na) are present in the system, since the latter two are the more stable chlorides. Again the situation changes when S is present. The stable form of S in oxidising conditions is SO_2/SO_3 which reacts with alkali and heavy metal chlorides to form sulphates releasing HCl. This in turn, will induce formation of $ZnCl_2$ and $PbCl_2$. The reduced form of S (H_2S) prevailing in reducing conditions was shown to have no influence on the volatility of the discussed heavy metals. Backman et al. [86] indicated further that the formation of Zn and Pb chlorides may be controlled by alkali and sulfur (ratios). The global equilibrium calculation showed that, in the case of refuse-fired boilers when alkalis, S, Cl and heavy metals are usually present, Zn and Pb will most likely condense first as sulphates and then as chlorides (on tube surface < 400 °C) while in reducing conditions the corresponding compounds are ZnO and PbS. This situation leads to the formation of a sticky, partly molten, corrosive deposit [18, 86]. Fluctuating conditions and continuously changing fuel composition may lead to aggressive conditions in waste-fired boilers.

2.5.3 Corrosion by Zn and Pb containing deposits

Zn and Pb corrosion has often been related to the formation of low-temperature melts that in combination with other elements from the deposit may act as a fluxing agent, leading to the dissolving of the protective oxide and resulting in severe corrosion [68, 88]. The presence of Pb and Zn chlorides was reported to decrease the first melting temperature of the deposit down to 200 °C - 300 °C, a factor which has been considered to have a significant influence on corrosion rates [9, 17, 20, 23, 24]. There have been very few studies handling the individual roles of Zn and Pb in the corrosion of boiler tube materials so the detailed corrosion mechanisms caused by those heavy metals have not yet been fully understood.

One of the first laboratory studies that investigated corrosion mechanisms in refuse-fired boilers was by Daniel et al. [68] and took place in the late 80's. In the experiments carbon and high-alloy steels were exposed to a 84$ZnCl_2$-16NaCl wt-% mixture at 316 °C temperature which approximated to the maximum surface temperature of the furnace wall tubes in one of the refuse fired boiler. The tested carbon steel corroded severely under the test conditions and the corrosion was estimated to be of several hundred mpy (milli inch per year, 1 mpy=0.025 mm/y). Based on the test results, the severe corrosion of the boiler materials by $ZnCl_2$ containing deposits were estimated to be mainly due to the presence of a liquid phase in the deposits and the fluxing (dissolving) of the protective oxide layer by the $ZnCl_2$ containing deposits. Also, the fluctuating conditions between reducing and oxidising were assumed to facilitate oxidation of formed $FeCl_2$ that could have resulted in the release of free Cl which could then be available for further reactions. In the following series of laboratory studies Daniel et al. [72] tried to identify particularly the corrosive constituents in deposits from refuse-fired boilers. Several salt mixtures composed of alkali chlorides, -sulphates, metal chlorides and Zn- and Pb chlorides and sulphates were prepared and tested at temperatures

representing the lower range of furnace wall surface temperature - (260 °C) and the upper range of superheater material temperatures - (566 °C). At 260 °C the heaviest attack was observed on carbon steel exposed to chloride mixtures containing also $ZnCl_2$, while the presence of $PbCl_2$ was found to have no evident effect on the corrosion rates at 260 °C. The important result was observed in tests at 566 °C, when the coupons of stainless steel TP304 were totally consumed by all the tested salt mixtures which contained $PbCl_2$ or $PbCl_2/PbSO_4$. Further, Miller and Krause [73] showed in their work that stainless steel corroded severely when exposed to $PbCl_2$ at 537 °C and to a somewhat lesser extent when exposed to $ZnCl_2$.

Lately, more detailed corrosion mechanisms describing the degradation of steels exposed to Zn- and Pb-compounds have been suggested. These studies were focused, however, mainly on salt mixtures containing $ZnCl_2$ (often KCl-$ZnCl_2$) [17, 22, 89-94], while only a little work has been done with $PbCl_2$ [17, 95, 96].

Spiegel [17] reported that experiments with pure $ZnCl_2$ and $PbCl_2$ at 500 ºC and 600 ºC (He-5%O_2, $H_2O<10^{-4}$bar) resulted in an enhanced degradation of 10CrMo9-10 and AC66 steels, while insignificant corrosion rates were measured at 400 ºC. Exposures of low-alloy steel to molten $ZnCl_2$ resulted in a formation of oxide layer consisting mainly of Fe_3O_4 and a $ZnFe_2O_4$ spinel. No fluxing of the scale was indicated. Similarly, also on an austenitic stainless steel (AC66) a Zn-rich spinel, (Fe, Zn)Cr_2O_3 was suggested to be a corrosion product. The suggested mechanism of formation was direct oxidation of $ZnCl_2$ and further reaction of ZnO with Fe_2O_3 (in the case of 10CrMo9-10 steel) or Cr_2O_3 (AC66) (reaction (10)):

$$ZnCl_2(l, s) + 1/2O_2(g) = ZnO(s) + Cl_2(g) \quad (10)$$

The enhanced corrosion of 10CrMo9-10 after exposures to $PbCl_2$ at 500 °C and 600 °C was described as occurring due to the presence of molten chloride. Precipitated Fe_2O_3 was observed in the corrosion products, so fluxing of the oxide scale by the $PbCl_2$ melt was suggested as a mechanism. On AC66 steel Fe_2O_3 and $PbCrO_4$ were listed as detected corrosion products. The formation of $PbCrO_4$ was described by reaction (11):

$$2PbCl_2(l) + Cr_2O_3(s) + 5/2O_2(g) = 2PbCrO_4(s) + 2Cl_2(g) \quad (11)$$

Li et al. [89] tested pure Fe, Cr, Ni and Fe-based (with different Cr content) alloys with a 55$ZnCl_2$-45KCl (mol%) mixture at 400-450 °C in pure O_2 which resulted in a heavy corrosion and the formation of a thick and porous oxide scale. The overall mechanism was the same as that stated by Spiegel [17] with the distinction that the reaction of oxidation of $ZnCl_2$ (reaction (10)) will produce a molten salt mixture enriched with KCl which was indicated to react with the Fe- and Cr-oxides present on the steels as in reactions (12) and (13).

$$4KCl(l) + 2Fe_2O_3(s) + O_2(g) = 2K_2Fe_2O_4(s) + 2Cl_2(g) \quad (12)$$

$$24KCl(l) + 10Cr_2O_3(s) + 9O_2(g) = 12K_2CrO_4(s) + 8CrCl_3(l) \quad (13)$$

The Cl_2 produced by reactions (11) and (12) dissolves into the salt and acts as an oxidant for Fe in all Fe-based materials; at the low oxygen partial pressure at the steel/salt interface Fe is

dissolved into the Cl containing melt and $FeCl_3$ (indicated by Spiegel [17] and Li et al. [89, 90, 93]) or $FeCl_2$ (Ruh et al. [97]) is formed (reactions (14) and (15)):

$$Fe(s) + 3Cl_2(g) = 2FeCl_3(diss) \quad (14)$$

$$Fe(s) + Cl_2(g) = FeCl_2(l) \quad (15)$$

Then the outward diffusion of the dissolved $FeCl_3$ or $FeCl_2$ with the subsequent oxidation occurs (reactions (16) and (17)). The outward diffusion of $CrCl_3$ and $NiCl_2$ is more restricted when compared to that of $FeCl_3/FeCl_2$ due to the limited solubility in the $ZnCl_2$-KCl melt. Therefore, according to Ruh and Spiegel [97], the solubility of metal chlorides in molten salts determines the extent of corrosion degradation of certain metals.

$$2FeCl_3(diss) + 3/2O_2 = Fe_2O_3(s) + 3Cl_2(g) \quad (16)$$

$$2FeCl_2(l) + 1/2O_2 = Fe_2O_3(s) + 2Cl_2(g) \quad (17)$$

The Cl_2 produced in reactions (16) and (17) was suggested to diffuse back to the metal/salt interface and to continue further chlorination of the metal [93, 97].

Further studies by Li et al. [90] with the same salt mixture (48$ZnCl_2$-52KCl, wt-%) at 400 °C and 450 °C (static air), but with the FeAl and NiAl alloys, showed that the corrosion resistance of the materials could be improved for high Al steels. The corrosion degradation for Al-bearing alloys in a $ZnCl_2$ containing environment was described as differing from Al-free alloys and to be due to the removal of Al by replacing it with $ZnCl_2$. The Zn^{2+} from the $ZnCl_2$-melt rather than Cl_2 or O_2 was indicated as the oxidant of Al.

Pan et al. [91] and Lu et al. [92] used the same salt mixtures as Li et al. [90] but the experiments were performed in a reducing atmosphere in the presence of HCl and H_2S gases. The scale developed in the atmosphere containing H_2S was thicker than the one developed in H_2S-free gases, but the composition of both scales was similar. The same mechanism as described by Spiegel [17] and Li et al. [89, 93] was proposed also in this case. Little was said about the corrosion products formed and about the direct influence of H_2S.

Otero et al. [95, 96] described the corrosion behaviour caused by a salt mixture containing $PbCl_2$ (52-48 mol% $PbCl_2$-KCl). They reported that the degradation rate of a 12CrMoV steel was so fast that the test specimens “disappeared” completely after 120 hr at 450 ºC and after 24 hr at 550 ºC. The corrosion rate of the superalloy IN-800 was shown to be remarkably lower at all tested temperatures (450-550 ºC).

Spiegel [88, 98] reported that the sulphates of Zn and Pb are less corrosive than their chlorides, though they have a strong influence on corrosion rates. The Zn and Pb sulphates were also found to decrease the melting point of the deposit in waste-fired boilers. He showed also that a mixture of Zn and Pb sulphates and sulphates of Ca, K and Na caused corrosion at 600 °C (in N_2-5%O_2) and that a sulphate melt containing the heavy metals was more corrosive than a mixture of only Ca, K, Na sulphates. The basic fluxing which causes dissolution of oxides into the sulphate melt was the proposed corrosion mechanism. The

analysis showed that most probably $ZnCr_2O_4$ was formed on a high Cr steel in the inner layer of the corrosion products demonstrating protection against further attack by sulphate melt. Inversely, on the iron-based steels the formation of highly soluble iron-oxides was observed. The formation of chromates was not observed. Also Fukusumi & Okanda [23] indicated that Zn sulphate may be equally or more corrosive than the corresponding alkali sulphates. It was shown that at 600 °C, for example, pure $ZnSO_4$ is equally corrosive as a mixture of Na_2SO_4-NaCl, and a mixture comprising of $ZnSO_4$-KCl caused more severe corrosion to carbon steel than a corresponding mixture of K_2SO_4-KCl.

The presence of Zn- and Pb-oxides in the salt mixtures/deposits has been discussed very briefly by Nakagawa & Matsunaga [99]. They investigated the effects of additions of ZnO and PbO to mixtures of NaCl-KCl and NaCl-KCl-Na_2SO_4-K_2SO_4 on corrosion at 550 °C. Both metal oxides caused accelerated corrosion of the tested alloys. It was suggested that if Zn and Pb oxides are present close to the metal surface they may be converted into their chlorides by free Cl_2 (the gas mixture contained 1000 ppm HCl). The presence of Zn- and Pb-chlorides caused an increase of the amount of melt in the salt mixture which enhanced the corrosion.

2.6 Concluding remarks on the literature

The combustion and co-combustion of waste-derived fuels has been reported to cause corrosion of boiler tube materials already at low waterwall temperatures. The corrosion was found to be related to the presence of Zn and Pb compounds in the deposits. The presence of Pb- and Zn-chlorides was reported to decrease the melting temperature of the deposit down to 200-300 ºC, a temperature range which has been considered to have a significant influence on the corrosion rates. In order to efficiently prevent corrosion or to be prepared for the failures it may cause, it is crucial to know how corrosive the elements present in the deposit and their compounds are. The corrosion induced by alkali chlorides (KCl, NaCl) which are usually present in significant amounts in waste fuels has been investigated in the literature quite extensively. However there is not so much literature available on high-temperature corrosion caused by the chlorides, sulphates or oxides of Zn and Pb. The problem of Pb and Zn rich corrosive deposit was brought up in several reports. The mechanisms suggested in the literature of corrosion caused by Zn- and Pb-chlorides containing ashes indicate that the main mechanism is the fluxing of the oxide scale by molten heavy metal chlorides. The subsequent chlorination of metal by the released chlorine continues the degradation of the steel. The Zn- and Pb-sulphates also decrease the melting point of the deposits and are equally corrosive as or more corrosive than the corresponding alkali sulphates. The fluxing of the oxide scale was also suggested to occur. The sulphates were shown, however, to start to become aggressive at higher temperatures than chlorides. Also, the oxides of Zn and Pb have been shown to cause corrosion. Exposures to salts containing $ZnCl_2$ and $ZnSO_4$ lead to the formation of Zn-Fe and Zn-Cr spinels, while the presence of Pb in a form $PbCl_2$ or $PbSO_4$ resulted in a Pb-Fe spinel and Pb-chromate. The presence of Pb was found to be especially aggressive against high chromium containing steels.

3. EXPERIMENTAL METHODS

In this section, the experimental methods and equipment used within this thesis are described.

3.1 Laboratory method for high-temperature corrosion tests

The thesis includes four papers in which a laboratory scale high-temperature corrosion test method has been used (**Papers I, II, III and VI**). The laboratory tests were performed to investigate the potential influence of Zn and Pb containing compounds/salt mixtures on high-temperature corrosion of typical boiler materials. Different superheater materials were selected and used in the experiments. The detailed compositions of steels are presented in *Section 4***.** The test specimens were machined to a size of approximately 20x20 mm and a thickness of 5 mm. Before the experiments, all steel specimens were polished in ethanol using first a 600 and then a 1000 grit SiC paper, then cleaned in an ultrasound bath and covered halfway or around the edges with a protective paste. The covering with the protective paste was incorporated in order to be able to determine the original surface after the corrosion tests and/or to prevent molten salt from flowing off from the sample's surface. Before the tests, the specimens were also pre-oxidised in a furnace for 24 h at 200 °C and then covered with a certain salt mixture (0.25g/specimen), which also can be thought to represent a simplified ash deposit (synthetic ash). After this the material samples (up to 5 at a time) were exposed at temperatures 250-600 °C in a horizontal tube furnace for 168 h (7 days), in an ambient or reducing atmosphere. The gas composition under reducing conditions was 5 vol-% CO and 95 vol-% N_2 with a total gas flow of 2.0 l/min at normal temperature and pressure (NTP). The chemical compositions of the salt mixtures used in the experiments are presented in *Section 4*. The corrosion furnace and the sample holder are presented in Figure 2. The salt mixtures were prepared by mixing together all the components, then the mixture was heated up until it fully or partially melted and cooled down to room temperature, when it was crushed and sieved to a size of 53-250 μm.

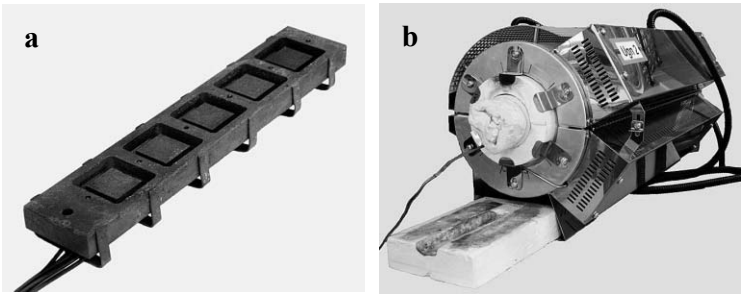

Figure 2. a) sample holder for exposure up to 5 samples at a time, b) horizontal tube furnace (courtesy Mr L. Silvander).

After the preparation process, the salt was analysed to check the influence of the heat pre-treatment on the salt composition. The aim of the pre-treatment was to homogenize the mixture. After the corrosion tests in an ambient atmosphere, the specimens were allowed to cool down to room temperature outside the furnace. The samples from tests in reducing atmosphere were cooled down to room temperature in a flowing N_2 gas. The samples were then placed in a

mould and cast in epoxy, then cut off in the middle to reveal the specimen's cross-section. The cross-section surfaces were further polished in kerosene, using 1000 and 1200 grit SiC paper, cleaned with petroleum ether in an ultrasound bath. Kerosene was used as a polishing lubricant in order to avoid dissolution of chlorine containing compounds. The samples were then analysed with Scanning Electron Microscope/Energy Dispersive X-ray (SEM/EDX) using backscatter electron mode to identify various chemical elements. The corrosion products were identified using X-ray images. The corrosion layer thickness was determined using SEM backscatter images. Several SEM images were combined into one panorama picture. The panorama pictures were then digitally treated by using contrast differences. An example of the treatment stages of a typical SEM panoramic picture is shown in Figure 3.

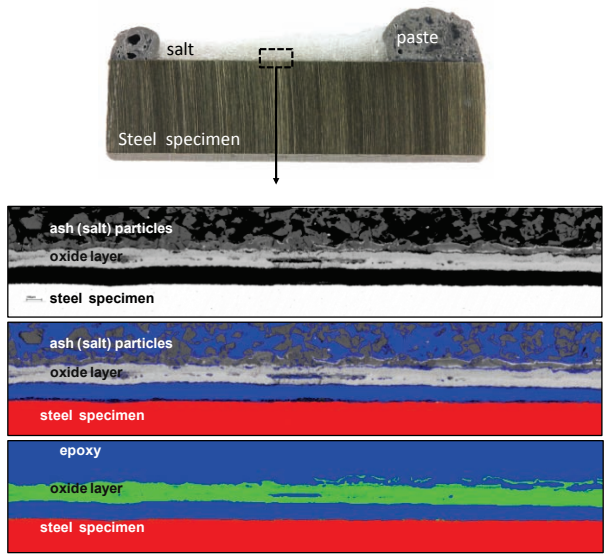

Figure 3. A steel sample cross-section and a schematic view of SEM pictures coloring stages in order to determine oxide layer thickness (Paper II).

After the panoramic images have been coloured, the thickness of the corrosion layer was determined for each vertical line of pixels and recalculated into µm [21,100]. The corrosion layer was defined as the thickness of the oxide layer, corrosion products (other than oxides) or degraded material for each line. In Figure 4a a schematic picture of a sample cross-section after a corrosion test with different types of corrosion is presented. Figure 4b shows the principle of thickness measurements of each of the corrosion layers. The final result was reported, depending on the type of the corrosion attack, either as the mean thickness of the individual layer or the total thickness (mean value) of affected region. To facilitate the analysis and the comparison of the results the certain ranges of the corrosion layer thickness were specified. The thickness ranges, however, should not be taken as exact but rather as indicative numbers:

- < 1 µm – insignificant corrosion
- 1-20 µm – detectable/low corrosion
- > 20 µm – significant corrosion
- > 60 µm – very high corrosion

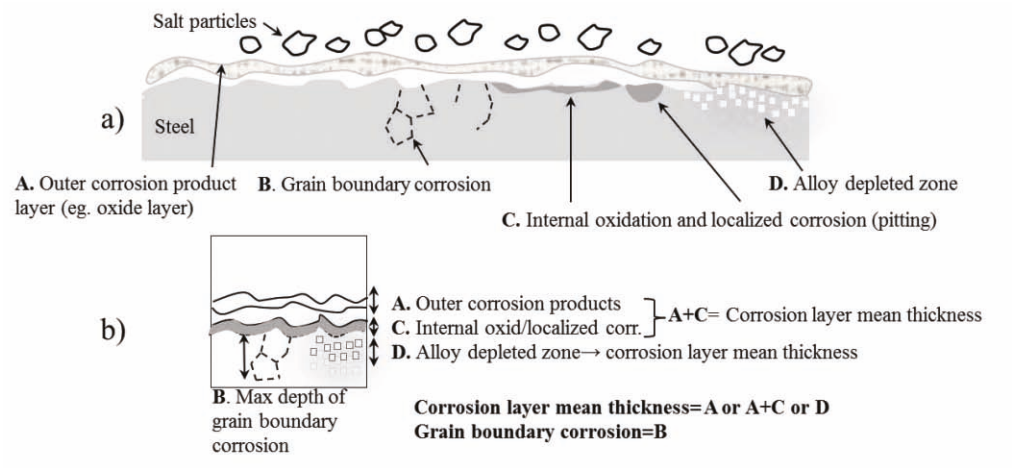

Figure 4. A schematic picture of a) a steel sample cross-section after a corrosion test and b) thickness measurement of corrosion layer.

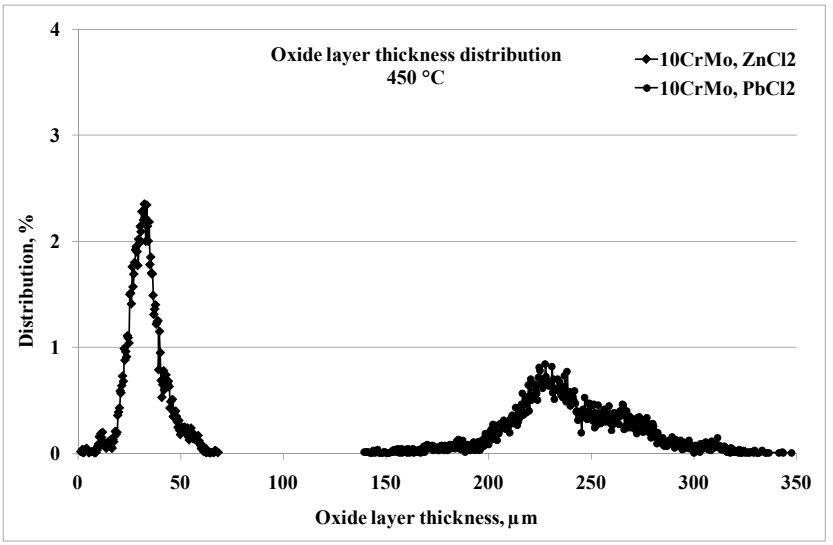

Figure 5. The oxide layer thickness distribution curves for 10CrMo9-10 steel exposed with $ZnCl_2$ and $PbCl_2$ at 450 °C (Paper I).

In Figure 5 the corrosion test results are presented as oxide layer thickness distribution curves. The curves show the distribution of the oxide layer thickness expressed as a percentage across the ~4 mm of the sample length. The shapes of the oxide layer distribution curve might be used to estimate the type of corrosion attack. For example the distribution curve achieved from the tests with $ZnCl_2$ (Figure 5, on the left) tends to fit to a relatively narrow, normal distribution curve. This indicates a relatively uniform corrosion attack. The distribution curve from the test with $PbCl_2$ (Figure 5, on the right) is flat and the data points are distributed widely. This results in a very uneven scale thickness and implies a strongly localized corrosion attack.

3.1.1 SEM-EDX

The metallographic cross-sections (**Papers I, II, III, VI**) as well as the cross-sections of the deposit samples (**Paper V**) were characterized with the use of a SEM - LEO Gemini 1530 with a Thermo Scientific UltraDry Silicon Drift Detector manufactured by Leo (2001) and EDX – ThermoNORAN Vantage X-ray analysing system manufactured by Thermo Scientific (2009). The SEM-EDX is an advanced analytical technique to characterize the elemental composition and surface structure of samples. The image of the sample is produced by scanning it with a high-energy beam of electrons in high vacuum. A highly focused beam of electrons emitted from an electron gun is accelerated towards the specimen. When electrons come into contact with the samples a complex series of interactions occurs. The sample-electrons interactions result in a variety of signals. These signals include secondary electrons (SE) that produce SEM images, backscattered electrons (BSE), characteristic X-rays (used for elemental analysis), visible light (cathodoluminescence - CL) and heat. Secondary electrons and backscattered electrons are commonly used for imaging samples. SE show the morphology and the topography of the samples, while BSE are most useful for illustrating contrasts in composition of the sample. In the backscattered electron mode, different elements are displayed with different darkness in the image; the heavier the element the lighter the colour [101]. The SEM images used in this work are mostly in a backscattered electron mode. Further, a new method (provided by Thermo Scientific) of identifying and visualizing sample areas of the same composition within a sample was used in **Papers III and V**. Using a collection of element maps for input – which may be elemental count maps, elemental quantitative maps, or component maps the software accurately identifies areas of about the same composition within the samples [102]. The oxide layer thickness and the thickness distribution on each specimen were evaluated based on the panorama SEM technique.

3.2 Bench-scale measurements

In **Paper IV**, high-temperature corrosion/deposit probe tests were carried out in a 30 kW_{th} BFB reactor firing wood pellets doped with $ZnCl_2$ in order to estimate the effect of Zn on high-temperature corrosion in waste wood fired boilers.

3.2.1 Bench-scale BFB reactor

The facility setup is shown in Figure 6. The reactor had a cylindrical shape with an inner diameter of 190 mm and a height of 550 mm. The freeboard section had a diameter of 310 mm and a height of 450 mm. At the bottom of the fluidization column a perforated plate (91 holes; diameter = 1.8 mm) was used for the distribution of fluidizing air. Sand (0.7-1.2 mm) was used as a bed material. The bed material was replaced with fresh sand before every new test. The fuel was fed from the top by means of a screw feeder together with the secondary air. During start-up, the bed was first heated to about 570 °C by electrical heaters which are lined around the reactor. The fuel feeding rate and the fluidization air were kept constant at 3 kg/h and 15 Nm^3/h respectively. The aim was to obtain a constant value of lambda (air-to-fuel ratio) of about λ=1.2. When the bed temperature reached 570 °C, the fuel feeding was started. Once the bed temperature reached a steady value and

the conditions were stable, the corrosion probe was introduced into the freeboard. The freeboard temperature was roughly 740-770 °C. The combustion conditions were kept constant for 7 h and then the probe was removed from the reactor. The gas velocity in the freeboard was about 0.5 m/s. The particulate matter was separated from the flue gases in the cyclone. After the cyclone before the stack, the flue gas was passed through a filter. The reactor temperatures, pressure drops in the bed, and air flows were monitored and recorded continuously during the experiments.

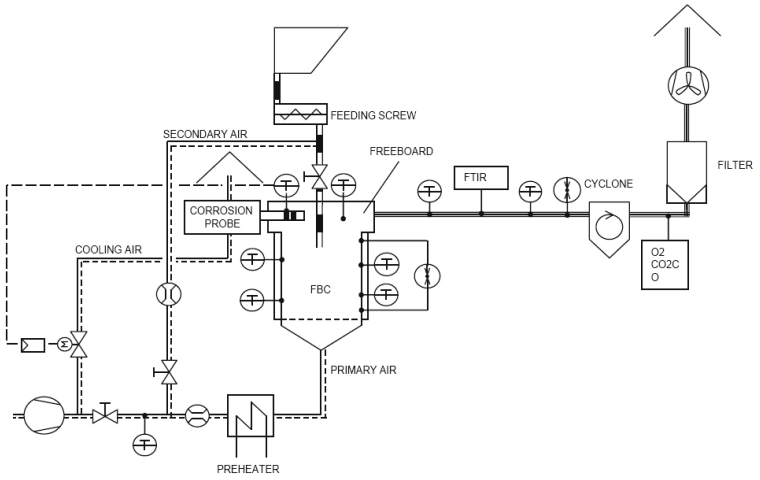

Figure 6. Setup of the 30 kWth fluidized bed reactor (Paper IV).

An air-cooled corrosion probe was used in the experiments. Temperature controlled probe techniques and examples of results that can be achieved with this kind of instrument have been described in detail by Laurén [103]. A schematic picture is shown in Figure 7. The probe was provided with two removable rings made of different steels. The temperature of one of the test rings on the probe was regulated with a PID-controller, adjusting the flow of the cooling air.

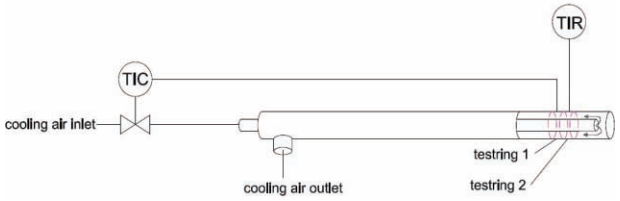

Figure 7. Outline of the corrosion/deposit probe (Paper IV).

The temperature of the other test ring was monitored and logged during the test run. Before the experiments, all steel rings were cleaned in ethanol using an ultrasound bath. After, the material rings (2 at a time) were fixed on the probe. The probe was preheated, prior to installation with a heating tape, to ~200 °C and introduced into the freeboard when the temperature in the freeboard exceeded 700 °C. Different probe cooling temperatures were set for each test (450 °C, 500 °C and 550 °C). After exposure, the test rings were cooled down to room temperature outside the furnace. The rings were then placed on a plate with a

small amount of resin thinned with acetone. The aim of thinning was to let the resin slowly penetrate the very thin layer of collected deposit, thus avoiding loosening the deposit into the resin. After drying, the rings were fully cast in resin and cut off in the middle, cleaned and polished. The treatment of the rings after the casting was followed-up by the same procedure as used in the laboratory-scale method (described in *Section 3.1*). The samples were then ready to be studied and analysed by SEM/EDX in order to identify the elemental composition of the deposit and to estimate the oxide layer thickness as a measure of corrosion.

3.3 Full-scale measurements

A measurement campaign discussed in **Paper V** was carried out at Stora Enso Anjalankoski co-incineration plant, in a BFB boiler co-firing solid recovered fuel with bark and waste-water sludge. The measurement campaign was carried out to determine the occurrence of Cl, Br, Zn and Pb in the fuel, in the combustion gases, as well as in the deposits on the boiler waterwalls. The results from the measurements campaign were complemented by thermodynamic calculations and laboratory tests (**Paper VI**).

3.3.1 BFB boiler

The capacity of Anjalankoski BFB boiler was 140 MW_{th}. The boiler's steam values were 80 bar/500 °C. The waterwall temperature in this boiler was estimated to be close to 350 °C. The boiler was utilising on energy basis 56% SRF - 37% bark - 7% sludge. The fuels were introduced into the boiler in separate streams. A schematic picture of the boiler with the feeding chutes, aerosol and deposit sampling locations and areas of highest corrosion (determined by Krautkramer USM 35X ultrasonic flaw detector) is shown in Figure 8.

3.3.2 Waterwall deposit sampling

Samples of deposits were collected by scratching from seven levels of the front (F1-F7) and the back (B1-B7) waterwalls. The sampling locations covered the corroded parts of both walls as well as the areas below and above and are marked by X in Figure 8. The collected samples (deposit flakes) were cast in epoxy and cut in the middle in order to reveal the deposits' cross-sections and to analyse the composition across the depth of the flakes. The distribution of the elements in the deposits was studied by SEM images and EDX analyses. The purpose of the deposit analyses was to identify the corrosive Cl-, Br-, Zn and Pb-compounds and to recognize eventual differences in the deposit compositions at different wall heights.

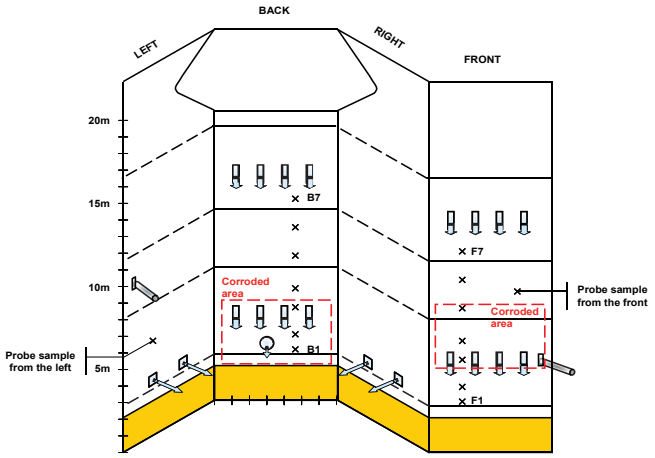

Figure 8. A schematic picture of the aerosol and deposit sampling locations (B1-B7 and F1-F7). The figure shows the four fuel feeding chutes on the left and right walls (4.5 m elevation), the sludge feeding through the back wall (4.5 m) and the eight air ports on the back and front wall (6 and 13 m elevations for secondary and tertiary air, respectively). The areas with the highest measured corrosion rates are marked with red dashed squares (Papers V & VI).

3.3.3 Aerosol sampling

Aerosol sampling was carried out with a combination of an air-cooled gas permeable tube probe and two consecutive ejector diluters. The gas sample was sucked into the probe, immediately diluted and quenched within a 200 mm long gas permeable tube diluter. The sample gas was taken from the probe to a second dilution stage and then divided between two parallel impactors: a Dekati-type Low Pressure Impactor (DLPI) and an Electric Low-Pressure Impactor (ELPI). A third gas stream was taken to an FTIR gas analyser. The setup also incorporated the use of a gas chromatograph (GC). Gas sample bags were filled with the gases ejected from the Fourier Transform Infra-Red (FTIR) analyser. The aerosol sampling setup is illustrated in Figure 9. The DLPI and gas sampling were carried out on the front and left walls of the BFB boiler. The purpose was to measure the conditions on the heavily corroding front wall and, for reference purposes, the non-corroding left wall area. These measurements were complemented by measurements at a third location at a distance of 1.5 m perpendicularly from the left wall towards the boiler centre (Figure 8).

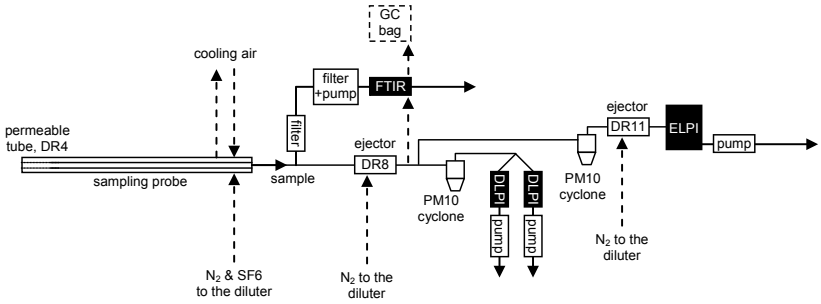

Figure 9. Schematic picture of the aerosol sampling installation (Paper V).

3.3.3.1 IC and ICP-MS (DLPI)

By means of the DLPI the aerosols (usually referred to in the literature as the particles with an aerodynamic diameter of approximately d_p<1μm) present in the combustion gases can be collected, and chemically analysed. DLPI is a cascade low-pressure impactor for classifying airborne particles into size fractions with evenly distributed impactor stages. The particles are collected on 25 mm collection membranes that are weighed before and after the measurement to obtain gravimetric size distribution of the particles [104]. The collection membranes were Nuclepore made of polycarbonate and greased with Apiezon L to facilitate particles adhesion [42]. The fine mode cut size in the DLPIs used in this work was d_p = 1.6 μm. The membranes with the collected particles (with d_p = 1.6 μm) were first extracted with water to determine water soluble elements. The SO_4^{2-}, Br^- and Cl^- were analysed by means of ion chromatography (IC) and the other water soluble elements by means of Inductively Coupled Plasma Mass Spectrometry (ICP-MS). As there were two DLPIs connected in parallel, the second DLPI membranes were extracted with HNO_3–HF and the solution was then analysed by means of ICP-MS for the total concentration of the elements.

3.3.4 Thermodynamic modelling procedure

In the thermodynamic equilibrium modelling a two-stage calculation procedure was applied to predict the forms of the ash forming elements. The conditions for the calculations were chosen to be similar to those occurring in the investigated BFB, as given in [10]. The fuel input is given in Table 2. The temperature of the combustion gases in the lower furnace approximated to 1100 °C, while the deposits on the waterwall had a temperature of 400 °C. The thermodynamic software package Factsage version 6.1 [105] was used for the modelling. The FACT53 database was used for the calculations of the stoichiometric condensed phases and the gas phase, while the SGTE database [106, 107] was used in the calculations of some gaseous heavy-metal compounds (e.g. SbCl, $PbBr_4$) that are not present in the FACT53 database. The only solution phases included were the rock salt-type alkali-halide solid solution (Na, K)(Cl, Br), and a liquid solution for molten salts containing Na^+, K^+, Ca^{2+}, Mg^{2+}, Zn^{2+}, Pb^{2+}//S^{2-}, SO_4^{2-}, CO_3^{2-}, Cl^-.

The vapour pressure and stability of various metal bromides and chlorides was also calculated. The chemical equilibrium at 1100 °C in both oxidising and reducing conditions was calculated in the first step. The equilibrium gas phase at 1100 °C was used as input for the second step (the condensed phases were removed from the input data for the second step) where, to simulate the formation of ash phases condensed from the gas phase, the equilibrium was calculated at 400 °C. The flow chart in Figure 10 describes the approach used.

Table 2. Composition of the fuel mix used in the thermodynamic equilibrium modelling (Paper VI).

Moisture (wt-%, ar)	36.5
Ash (wt-%, ds)	9.9
IN DRY SOLIDS (wt-%)	
C	52.2
H	7.1
N	1.0
S	0.16
O	29.2
IN DRY SOLIDS (mg/kg)	
Cl	5 280
Br	80
Na	1 860
K	1 470
Ca	16 910
Mg	1 260
P	500
Al	1 900
Si	9 090
Fe	2 080
Ba	170
Sb	150
Cr	40
Cu	140
Pb	70
Mn	160
Ni	10
Zn	280
Sn	5
HEATING VALUE (MJ/kg)	
LHV, db	21.1
LHV, ar	12.5

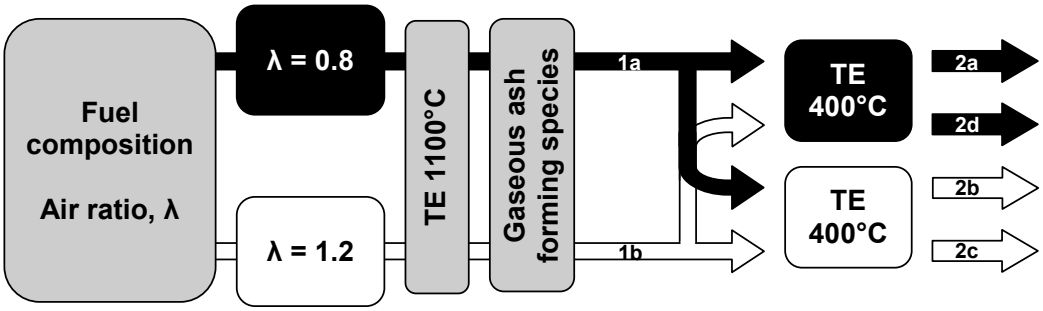

Figure10. Flow chart describing the calculation procedure, λ = air ratio, TE = thermodynamic equilibrium (Paper VI).

Two main cases were considered:

2a: cooling of the 1a gas phase formed at reducing conditions (λ=0.8) from 1100 °C to 400 °C

2b: cooling of the 1a gas phase formed at reducing conditions (λ=0.8) from 1100 °C to 400 °C and adding air to correspond to 3 vol-% O_2 in the equilibrium gas phase

2c: cooling of the oxidized gas 1b from 1100 °C to 400 °C

2d: cooling of the oxidized gas 1b from 1100 °C to 400 °C and setting activity of O_2 to correspond to the reducing conditions in 2a

The results from cases **2c & 2d** did not show any significant differences, and are not discussed.

4. RESULTS AND DISCUSSION

The following chapter gives a summary of the main results on corrosion of boiler tube materials in environments rich in Zn and Pb. It discusses the main findings on the subject starting from the laboratory test results, through the bench-scale measurements and ends with full-scale measurements complemented by thermodynamic modelling.

4.1 Corrosion laboratory tests with Zn- and Pb-containing synthetic deposits

Deposits in waste-fired boilers contain significant quantities of heavy metals such as Zn and Pb [7, 9, 10, 12, 14, 17, 20, 25, 40, 63, 65]. Different forms of Zn and Pb may be found in deposit from different areas of the boiler and of the convective sections. In this part well-controlled laboratory tests were carried out (**Papers I, II & III** and partially **Paper VI**). The aim of the laboratory tests was to get better understanding of the corrosion tendencies of Zn and Pb containing compounds and to gain better knowledge of the corrosion mechanisms under exposure to those compounds. The detailed compositions of all tested materials are presented in Table 1 in *Section 2.2*.

4.1.1 Tests with single salts; $ZnCl_2$, $PbCl_2$, ZnO and PbO

In **Paper I** the corrosiveness of:

- $ZnCl_2$ (melting temperature (T_m)=318 °C)
- $PbCl_2$ (T_m=501 °C)
- ZnO (T_m=1975 °C)
- PbO (T_m=888 °C)

was tested on one low-alloy (10CrMo9-10) and on one stainless steel (AISI 347). Simple systems were used in order to investigate the corrosion tendency and mechanisms of these specific heavy metals. Figure 11 shows the resulting mean oxide layer thicknesses in both steels after exposure to the above-mentioned compounds at different temperatures. For heavy metal chlorides the selected test temperatures were below and above their melting temperatures. The oxides, due to their high melting temperature, were tested at just one temperature, 550 °C. Additionally, results from tests without any salt compound were used as a comparison.

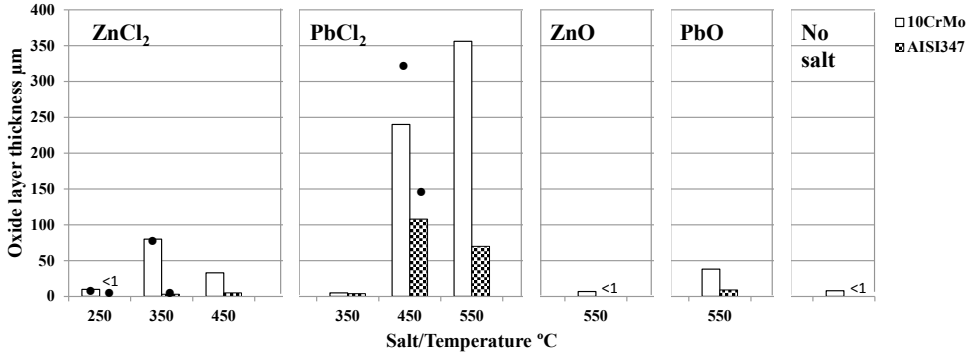

Figure 11. The oxide layer thickness measured on 10CrMo9-10 and AISI 347 after 168 h exposures to $ZnCl_2$, $PbCl_2$, ZnO and PbO at 250-550 °C. The "•" sign stands for results from repetition tests (Paper I).

The exposures of 10CrMo9-10 steel to $ZnCl_2$, resulted in a significant corrosion already at 350 °C (80 µm). At 450 °C the oxide layer on 10CrMo9-10 being slightly thinner than at 350 °C was explained as being caused by faster evaporation of $ZnCl_2$. After the test, $ZnCl_2$ was not detected on the steel sample at 450 °C. The stainless steel did not corrode in the presence of molten $ZnCl_2$, and the good resistance was assumed to be due to the protective Cr_2O_3 which acted as a shield against chlorides.

In the tests with $PbCl_2$ extreme corrosion was observed on both the low-alloy and the stainless steel already below the melting temperature of $PbCl_2$. This significant damage was observed at 450 °C. The significant corrosion on the stainless steel exposed to $PbCl_2$ was assigned to the formation of $PbCrO_4$. The formation of $PbCrO_4$ destroys the integrity of Cr_2O_3 enabling the formation of metal chlorides and further destruction of the metal surface. The described reaction is considered to resemble the reaction between KCl and Cr_2O_3 resulting in a K_2CrO_4 formation described earlier by Li et al. [108], Petterson et al. [109] and Lehmusto et al. [110]. The different situation was observed when high Cr steels were exposed to $ZnCl_2$. Zn did not form chromate and thus the protective abilities of Cr_2O_3 were maintained.

The SEM-EDX analyses showed that exposure to both chlorides caused formation of metal chlorides ($FeCl_2$, $CrCl_2$) on the steel surfaces. Apart from that, it was observed that the main corrosion products on 10CrMo9-10 were Fe_xO_y and $ZnFe_2O_4$ in contact with $ZnCl_2$ and Fe_xO_y, and $PbFe_2O_4$ in contact with $PbCl_2$. While on AISI 347, the Fe_xO_y and $PbCrO_4$ were found to be the prevailing corrosion products of the steel/$PbCl_2$ reaction. These compounds were assumed to be present based on atomic ratios.

The oxide layer developed on 10CrMo9-10 after exposures to ZnO at 550 °C was of the same thickness as after exposure with no salt and was of just few µm thick. It means that the ZnO had not interacted with the steel at the tested conditions of 550 °C and the developed oxide layer results from the normal oxidation in air. The oxide layer on AISI 347 was under the detection limit of the method used. The tests with PbO were also performed only at 550 °C and resulted in heavy corrosion on the 10CrMo9-10 and just a moderate oxide layer growth on the AISI 347. It was assumed that during the exposures to PbO the stainless steel experienced formation of $PbCrO_4$ (based on atomic ratios). In order to confirm also the

formation of lead chromate via the reaction of Cr_2O_3 with metallic Pb, a mixture of Cr_2O_3 and Pb (50/50 wt-%) was heat treated at 450 ºC for 96 h. The products identified by the XRD (X-ray diffraction) contained unreacted Pb and Cr_2O_3 and also some $PbCrO_4$ and PbO. The same test was performed with a Cr_2O_3+$PbCl_2$ mixture. The XRD identified products contained mainly $PbCrO_4$ and small amounts of Cr_2O_3 and $PbCl_2$.

The damage of Cr_2O_3 by Pb-compounds (e.g. $PbCl_2$, Pb, PbO) is considered to be the first step in the corrosion process under $PbCl_2$ and proceeds according to reaction (11) presented in *Section 2.5.3*, described also by Spiegel [17].

While in the tests with $ZnCl_2$, fast evaporation occurred at the tested temperatures and only limited amount of $ZnCl_2$ had time to react. The earlier described corrosion products formed via the contact of $ZnCl_2$ with low-alloy steel surface could have resulted from the following chain of reactions: relatively fast oxidation of molten $ZnCl_2$ (reaction (10), *Section 2.5.3*) [111] and simultaneous reaction with Fe_3O_4 (which covers the steel surface) resulting in a $ZnFe_2O_4$ and $FeCl_2$ formation (reaction (18)). The Fe_3O_4 layer destroyed by reaction (18) opens a path for free Cl_2 from reaction (10):

$$ZnCl_2(l) + Fe_3O_4(s) \rightarrow ZnFe_2O_4(s) + FeCl_2(s) \quad (18)$$

In a real case, the Cl_2 formed in reactions (1) and (2) is expected to be partially converted to HCl due to the presence of some H_2O in the combustion gases and released to the gas phase. However, some amount of Cl_2 is regarded as being available for subsequent chlorination of the metal which took place as described earlier.

Thermodynamic equilibrium calculations were made in order to support the empirical data achieved from the laboratory test, and especially those concerning the volatility of $ZnCl_2$ and $PbCl_2$. Figure 12 presents the saturation pressure for both chlorides at tested temperatures. The saturation pressure of $ZnCl_2$ at 350 °C is 85 ppm while at 450 °C it is already almost 3000 ppm at the test conditions. This corresponds well with the situation observed during the tests where only very small amounts of $ZnCl_2$ could be detected after the treatment at 350 °C. A similar conclusion can be applied to $PbCl_2$ where a corresponding behaviour was observed at temperatures of about 100 °C higher meaning that at 450 °C the saturation pressure of $PbCl_2$ was significantly lower (50 ppm) than at 550 °C (1300 ppm). Further, no $PbCl_2$ was detected on the steel samples after the test at 550 °C.

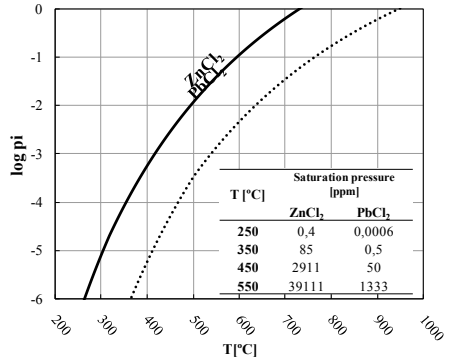

Figure 12. Saturation pressure curves for $ZnCl_2$ and $PbCl_2$ at 250, 350, 450 and 550 °C (Paper I).

Oxide layer distribution curves were used to suggest the type of corrosion attack. Figure 13 shows two examples after exposing AISI 347 to $ZnCl_2$ and $PbCl_2$ at 450 °C. The distribution curve obtained from the test with $ZnCl_2$ tends to fit to a relatively narrow normal distribution curve, indicating a relatively uniform corrosion attack. The distribution curve of the $PbCl_2$ test is flat and the data points were distributed widely. This is the result of a very uneven scale thickness and implies localized corrosion (Figure 13).

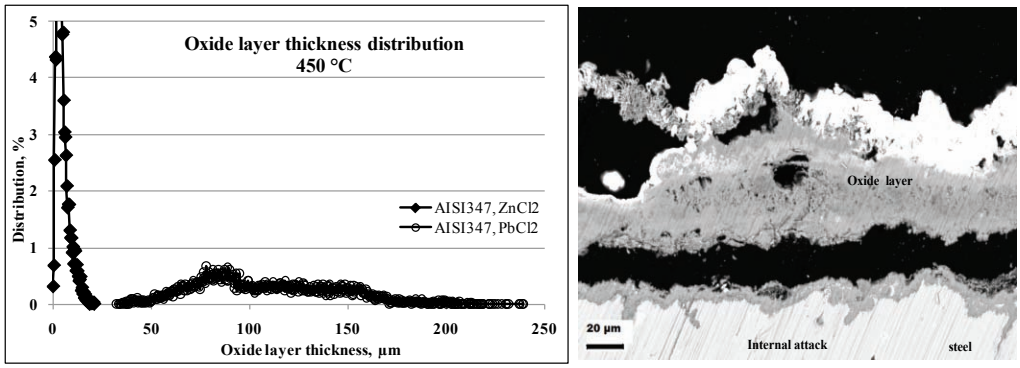

Figure 13. The oxide layer thickness distribution curves for AISI 347 steels exposed to $ZnCl_2$ and $PbCl_2$ at 450 ºC and the localized, internal attack on the AISI 347 steel after 168 h exposure with $PbCl_2$, 550 ºC (Paper I).

4.1.2 $ZnCl_2$ and $PbCl_2$ containing mixtures

The aim of testing pure Zn and Pb chlorides and oxides was to obtain better understanding of the corrosion mechanisms and to determine how (synthetic) deposits containing the mentioned compounds may affect the performance of the boiler tube materials. **Papers II & III** describe results from tests with salt mixtures containing Zn and Pb chlorides. The detailed compositions of tested salts and the salt mixtures are shown in Table 3.

Table 3. The compositions of the salts and the salt mixtures (wt-%) (Paper III).

	$ZnCl_2$	$PbCl_2$	KCl	K_2SO_4	Melt fraction*		
					400 °C	500 °C	600 °C
Salts from paper III	5	5	90	0	18	19	22
	0	5	95	0	0	7	8
	0	5	0	95	0	5	6
	0	100	0	0	0	0-100**	100
Salts from paper II	0	0	0	100	0	0	0
	5	0	0	95	13	15	17
Salt from paper XIII	0	0	100	0	0	0	0

*- At designated temperatures and at test conditions

** - Due to the very small difference between the melting temperature of $PbCl_2$ and the test temperature (longitudinal temperature gradient in the oven) the melt fraction cannot be indicated precisely

Figures 14a, 14b & 14c show the resulting mean corrosion layer thickness of both steels after exposures to the single salts of $PbCl_2$, KCl and K_2SO_4 and to the $PbCl_2$- and $ZnCl_2$-containing salt mixtures at 400 °C, 500 °C and 600 °C. At the lowest test temperature (400 °C), the highest corrosion was observed on both test materials when both $PbCl_2$ and $ZnCl_2$ were present in the mixture with KCl. Such a strong attack on the low-alloy steel and fairly high degradation of the austenitic stainless steel may be due to the presence of the molten phase which comprised nearly 20% of the salt mixture at 400 °C. The $PbCl_2$-$ZnCl_2$-KCl mixture contained the highest fraction of melt out of all tested salt mixtures at all test temperatures, but the degradation of the steel by this salt mixture was not the highest at all test temperatures. This observation demonstrates that, in these tests, the amount of melt does not necessary decide the corrosion level. All salts containing $PbCl_2$ caused extreme corrosion at 500 °C and above, reaching in the case of 10CrMo9-10 a corrosion layer thickness of 250 µm. The results obtained are dramatic, taking into account that the $PbCl_2$ content was only 5 wt-% of the salt mixture. Both materials were severely corroded and the extent of damage observed on AISI 347 was surprisingly near to the levels measured on low-alloy steel (10CrMo9-10). The extent of corrosion from the tests with $ZnCl_2$-K_2SO_4 was below 50 µm for both tested materials, which already is a significant result. The AISI 347, though not free from defects, showed much better resistance in the presence of $ZnCl_2$-containing mixtures. At 600 °C, the corrosion caused by the salts containing $PbCl_2$ was severe and the levels of degradation were very similar. In addition, only very small differences were observed in the corrosion layer thicknesses on both materials. In the majority of other tests the difference between the corrosion layer thicknesses of 10CrMo9-10 and AISI 347 was rather evident. The $ZnCl_2$ containing salts were less aggressive with the AISI 347 in comparison to $PbCl_2$ salt mixtures. Thus, it can be pointed out that at temperatures ≥500 °C in an environment containing $PbCl_2$ the austenitic stainless steel AISI 347 (with 18 wt-% of Cr) may not be suitable.

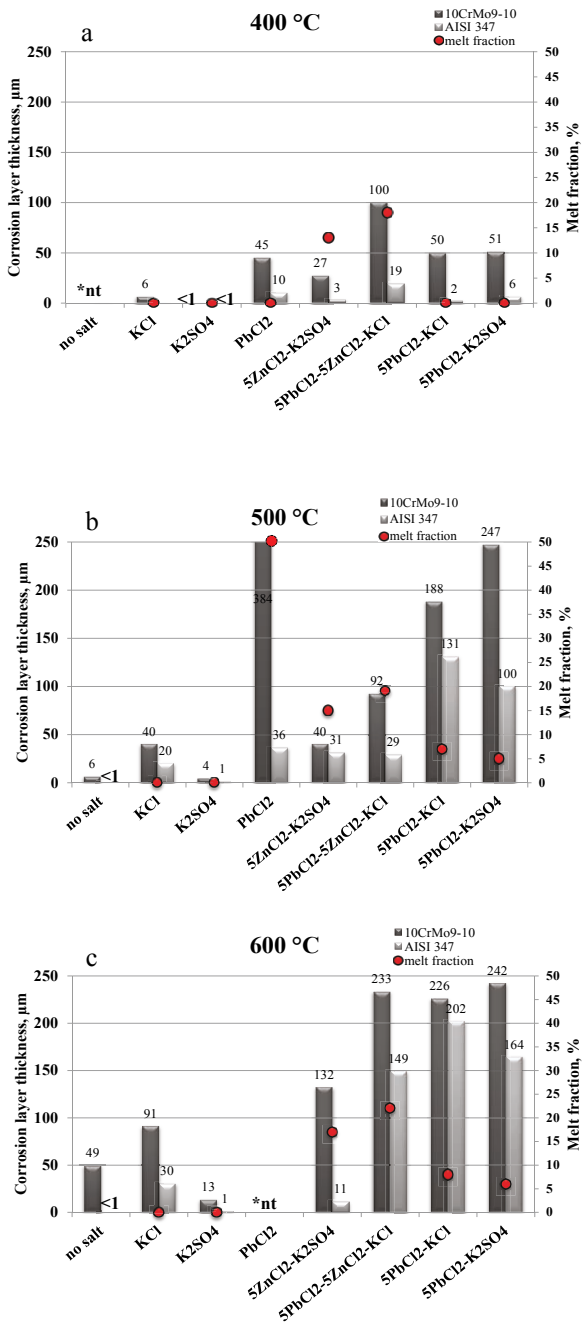

Figure 14. The corrosion layer thickness measured on 10CrMo9-10 and AISI 347 steels after 168h exposures to salts containing different amounts of $PbCl_2$-$ZnCl_2$-KCl-K_2SO_4 at 400 °C - 600 °C. *nt – not tested. The calculated melt fraction for the tested salt mixtures is also included in the graph (Paper III).

Analysis of the steel samples exposed to $ZnCl_2$ containing mixtures revealed that already at 400 °C the areas on the alloy/oxide scale interface were rich in Cl and Fe in case of low-alloy steel, and Cl and Cr rich when high Cr steel was exposed. Smaller amounts of S, Zn, and K were also detected. These results indicate that the volatile metal chlorides (particularly $FeCl_2$) play a key role already at 400 °C. The literature [17, 79, 81] describes the chlorination of iron and/or chromium taking place on the steel surface, the formed $FeCl_2$ and $CrCl_2$ volatilizing (due to their high vapour pressure) towards the oxide scale/gas interphase where higher concentration of oxygen causes oxidation of the metal chlorides to metal oxides. The oxide layer formed via oxidation of the metal chlorides is porous and provides no protection to the metal.

Figure 15 shows SEM panorama pictures of 10CrMo9-10 steel after exposures to $PbCl_2$-$ZnCl_2$-KCl, $PbCl_2$-KCl, and $PbCl_2$-K_2SO_4 salt mixtures at 500 °C. The addition of $ZnCl_2$ to the $PbCl_2$-KCl mixture decreased the solidus temperature (T_0) of the salt mixture but also the amount of melt (Figure 14 b). The salt particles were clearly fused. It was not observed in the cases with the two other mixtures without the presence of $ZnCl_2$, even though the lowest solidus temperature for a $PbCl_2$-KCl mixture and a $PbCl_2$-K_2SO_4 mixture according to the literature are 411 °C [112] and 403 °C [113] respectively. The addition of $ZnCl_2$ to the $PbCl_2$-KCl mixture caused the highest degradation of the materials at 400 °C most likely also due to the presence of higher amount of melt.

Figure 16 presents a SEM picture of 10CrMo9-10 steel after exposure to a $PbCl_2$-KCl mixture at 500 °C and the areas (also called *phases*) with about the same elemental composition as identified by applying Xphase spectral imaging software. The top most part of *phase a* was composed entirely of Fe and O. The lower parts (*phase b*) of this Fe_xO_y contained additionally traces of Cr, Cl and K, which were not observed in the top most part of the layered Fe_xO_y. The lack of elements originating from the salt in the top most part of the scale suggests that oxide was formed via the oxidation of metal chlorides which were formed during the exposure.

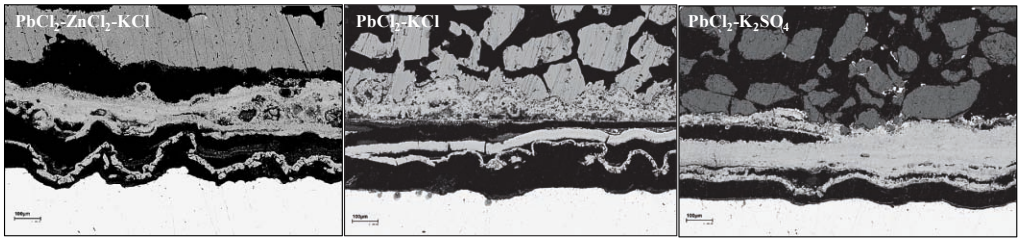

Figure 15. SEM pictures of 10CrMo9-10 after 168 h exposure with $5PbCl_2$-$5ZnCl_2$-KCl, $5PbCl_2$-KCl, $5PbCl_2$-K_2SO_4 (wt-%) at 500 °C (Paper III).

The formation of $FeCl_2$ that was observed on the steel surface is supported by the composition of *phase d*. $FeCl_2$ was present on the low-alloy steel surface at all three tested temperatures. But also after exposures with $PbCl_2$-$ZnCl_2$-KCl mixture, the surface of the metal was rich in Cl and Fe. The upper part of the middle oxide (*phase c*) stands probably for the original surface of the sample. The analysis showed that the layer is enriched with salt elements like K and Cl and a smaller amount of Pb. The simultaneous presence of K and Pb together with Cr, suggests that small amounts of $KCrO_4$ and/or $PbCrO_4$ most probably were formed.

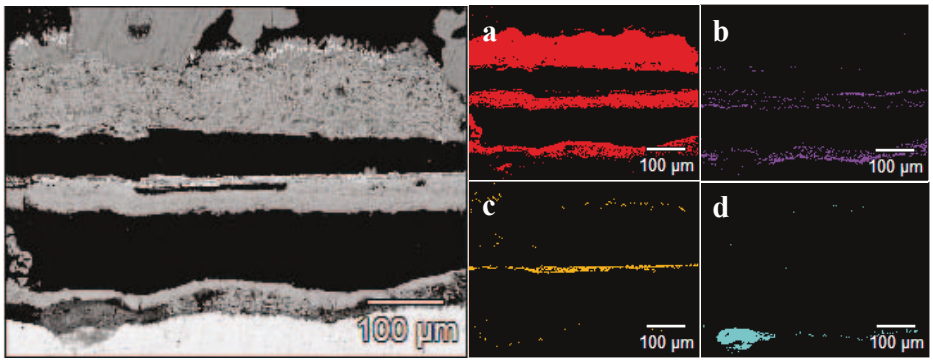

Atomic %	O	Fe	Cr	Cl	K	Pb
Phase a	57	41	<1	<1	<1	-
Phase b	52	38	5	2	1	-
Phase c	50	20	4	10	12	2
Phase d	52	32	2	19	-	-

Figure 16. Individual Xphase maps and atomic % of the elements in the corrosion products on the 10CrMo9-10 steel after 168 h exposures with $PbCl_2$-KCl at 500 °C (Paper III).

The surface of the samples exposed to $PbCl_2$-K_2SO_4 was apart from Cl and Fe enriched with S. Additionally grain boundary corrosion was observed at all test temperatures.

4.1.3 $ZnCl_2$-K_2SO_4 and $ZnBr_2$-K_2SO_4

At the time of compiling the results of this thesis, experimental results on the differences in the corrosiveness between heavy metal chlorides and bromides that can be part of ash deposits in certain environments were not available. Further, the literature handling bromine-related high-temperature corrosion was scarce. The possible influence of bromine on corrosion in waste incinerators was brought up by Rademakers et al. [70] and later bromine-induced corrosion was discussed by Vainikka et al. [10] and their work added impetus to the performing of experiments in which instead of Cl, the effect of the presence of Br was investigated. **Paper VI** reports, among other, the degree of corrosion of boiler steels exposed to zinc bromide containing salt mixtures. The results were further compared to the corresponding zinc chloride containing mixtures.

The detailed compositions of the tested materials are shown in Table 1 in *Section 2.2*. Since the waterwalls of the boiler (in which the bromine corrosion was observed) were exposed to fluctuating conditions, the laboratory tests were performed in both an oxidizing (ambient air) and a reducing atmosphere (5CO-95N_2 vol-%; gas flow - 2.0 l/min, NTP). The waterwall temperature was estimated to be around 350 °C so just two test temperatures, 350 °C and 400 °C, were chosen for detailed discussion here. The tests in oxidizing conditions were also performed at 500 °C and 600 °C.

The chemical composition of the salt mixtures used in tests was as follows:

- 6 mol% $ZnBr_2$ – 94 mol% K_2SO_4
- 6 mol% $ZnCl_2$ – 94 mol% K_2SO_4

Figure 17 presents the average corrosion layer thickness for the steels tested with the $ZnBr_2$ and $ZnCl_2$ containing salt mixtures. At 350 °C, a thin oxide layer was developed on the low-alloy steels while the oxide layer thickness on both austenitic steels was under the detection limit. When the temperature was increased to 400 °C all the materials experienced similar oxide layer thickness growth (12-16 µm) at reducing conditions. The mixture with $ZnBr_2$ was found to be more aggressive at 400 °C in oxidising conditions than the corresponding mixture with $ZnCl_2$. The heavy corrosion measured on 10CrMo9-10 exceeded significantly the attack caused by the salt containing $ZnCl_2$. Also, for AISI 347 resistance deteriorated in the presence of zinc bromide.

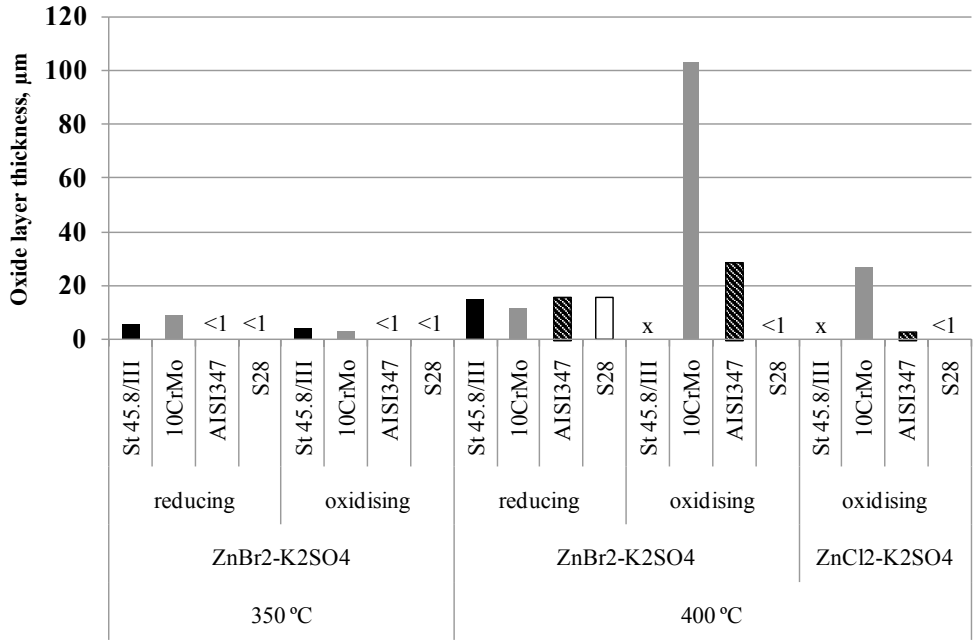

Figure 17. Oxide layer thicknesses measured on tested steels after 168 h exposures in air and in reducing atmosphere with 6 mol-% $ZnBr_2$+K_2SO_4 and 6 mol% $ZnCl_2$+K_2SO_4 mixtures at 350 °C and 450 °C. The x's mean that the test was not performed (Paper VI).

At 400 °C an internal degradation of 10CrMo9-10 together with an oxide layer growth was observed. The steel surface was bromine rich indicating the formation of $FeBr_2$ (Figure 18). At 500 °C, as described in details in **Paper VI,** a clear decomposition of $ZnBr_2$ and a formation of KBr was observed.

It has been suggested [114] that at higher temperatures, similarly to chlorides, active oxidation is a prevailing type of corrosion responsible for the degradation of metals in the Br-rich environment. It is therefore expected that the reactions of metals such as Fe with Br species will be analogous to those with Cl. HBr(g), or rather Br_2(g), may diffuse through the oxide scale to the metal surface. The analogous reactions with HCl and Cl_2 were described by

Grabke et al. [79], Spiegel [17] and Zahs et al. [115]. Additionally, the metal surface can also simultaneously undergo direct reaction with a Br containing salt/deposit. As a result, highly volatile $FeBr_2$, destroying steel will be formed.

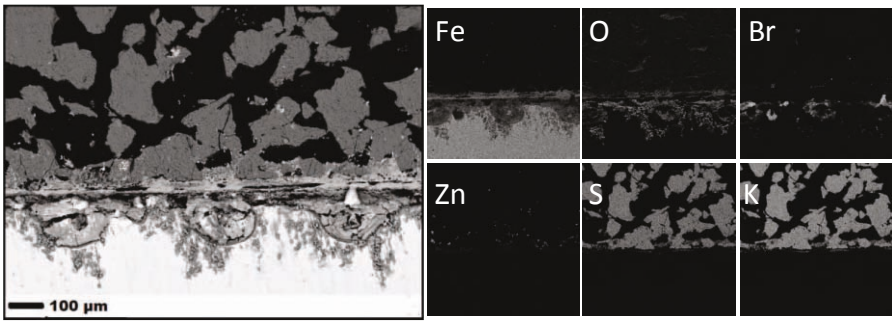

Figure 18. SEM image and X-ray maps of the 10CrMo9-10 steel after 168 h exposure with 6 mol-% $ZnBr_2$+K_2SO_4, 400 °C (Paper VI).

Since $FeBr_2$ has a slightly higher vapour pressure than $FeCl_2$ and the partial pressure $p(O_2)$ required to oxidize $FeBr_2$ to Fe_2O_3 at 400 °C is noticeably lower than for $FeCl_2$, $FeBr_2$ will be oxidized closer to the steel surface. This situation can be observed from the phase stability diagrams for the Fe-Br_2-O_2 and Fe-Cl_2-O_2 systems at 400 °C (Figure 19). In practice this means that Br_2 or HBr will be released close to the steel surface and a large fraction may still be available for further reactions with the metal, thus causing more severe corrosion.

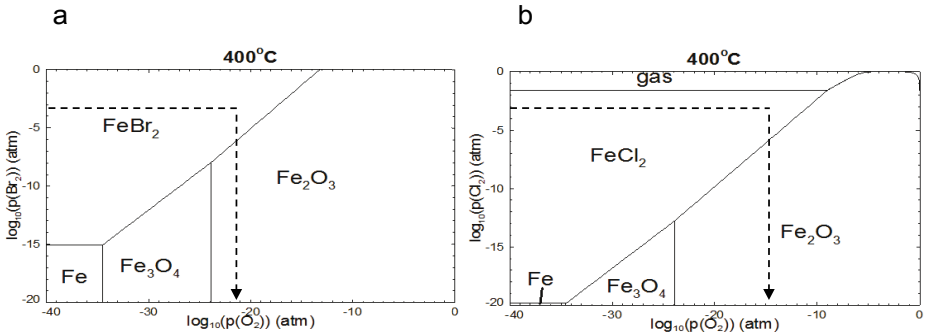

Figure 19. Phase stability diagrams for a) Fe-Br_2-O_2 at 400 °C, b) Fe-Cl_2-O_2 at 400 °C systems (Paper VI).

In contrast, $FeCl_2$ is more stable and will diffuse further out through the deposit before the required amount of O_2 needed for oxidation is present. Such behaviour may lead to the situation that a larger amount of Cl, than of Br, may be released from the deposit into the flue gas.

In the tests in a reducing atmosphere, the formed corrosion layer was different in composition when comparing to what was observed under oxidising conditions. The oxide layer was composed mainly of Fe, Zn and S and was slightly thicker in places where the salt particles were in a direct contact with the steel surface. Otherwise the corrosion layer was quite thin, and even (Figure 20). These results correlate very well with the thermodynamic predictions (presented in *Section 4.3.3*) which showed that in reducing conditions sulfur should mainly

form Zn, Pb and Fe sulphides in the deposits. The formation of a Fe-Zn-S system with some oxygen was clearly observed (Figure 20).

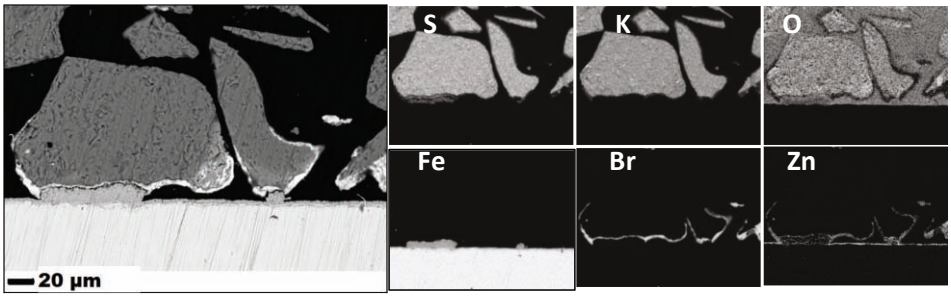

Figure 20. SEM image and X-ray maps of the St 45.8/III steel after 168h exposure with 6 mol-% $ZnBr_2$+K_2SO_4 at 350 °C in reducing atmosphere (Paper VI).

4.2 Corrosion during firing of wood pellets doped with $ZnCl_2$

Waste wood is usually substantially contaminated with trace elements and heavy metals such as Zn. It may cause slagging, fouling, and corrosion of the boiler's heat exchanging surfaces. Heavy metal compounds, such as $ZnCl_2$ decrease the first melting point of a deposit, and that can induce corrosion, especially by molten salts [17].

To study the general impact of firing waste wood containing higher amounts of Zn and Cl, and to evaluate the role of $ZnCl_2$ in high-temperature corrosion, a series of corrosion probe tests were carried out in a 30 kW_{th} bench-scale fluidized-bed reactor firing doped wood pellets (**Paper IV**). Two types of wood pellets were burnt in the reactor: one doped with $ZnCl_2$ and an untreated one as a reference. The solid $ZnCl_2$ was first dissolved in ion exchanged water and the solution was then carefully sprayed on the wood pellets using a sprinkler and left to dry. The wood pellets were then packed in tightly closed barrels. The amount of Zn in the doped pellets (2170 mg/kg) corresponded to a high level of Zn in waste wood [40]. The amount of Cl added through the doping (1380 mg/kg) resulted in a higher level of Cl than usually found in waste wood, but waste wood fractions with higher Cl content are also often present [116]. The performed tests are listed in Table 4..

Table 4. List of performed tests (Paper IV).

Experimental Part	Fuel	Exposure time (h)	Steel	Probe temp. (°C)
A	wood pellet doped with $ZnCl_2$	7	10Cr-Mo9-10 S28	550
	wood pellet doped with $ZnCl_2$	7	10Cr-Mo9-10 S28	550
	wood pellet doped with $ZnCl_2$	7	10Cr-Mo9-10 S28	500
	wood pellet doped with $ZnCl_2$	7	10Cr-Mo9-10 S28	450
B	wood pellet	7	10Cr-Mo9-10 S28	550
	wood pellet	7	10Cr-Mo9-10 S28	500
	wood pellet	7	10Cr-Mo9-10 S28	450

Tests were performed using pure wood pellets as a reference and wood pellets doped with ~0.5 wt-% $ZnCl_2$. The probe exposures lasted for 7 h while the test ring temperatures were 450 °C, 500 °C and 550 °C.

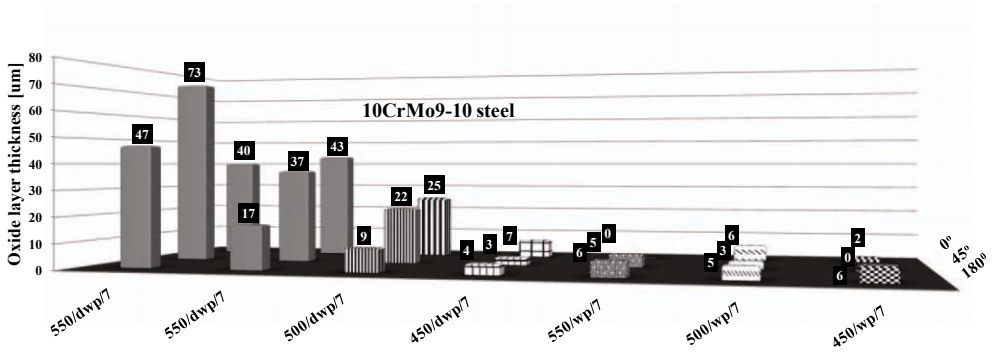

Figure 21. Oxide layer thickness of the rings analyzed and measured by means of SEM. Abbreviations on the X-axis stand for test conditions: temperature of the rings, °C / dwp-doped wood pellet or wp-wood pellet) / probe exposure time, h (Paper IV).

A summary of the corrosion layer thicknesses at 0°, +/- 45° and 180° angles (0°- windward side i.e. the side against the flue gas stream, +/- 45° angle from the windward side, 180°- leeward side) of the steel rings are presented in Figure 21.

The austenitic stainless steel Sanicro 28 showed good resistance under all test conditions and the oxide layer was under the detection limit (<1µm). For 10CrMo9-10 the thickest oxide layer was measured on the windward section (0° - 45°) of the probe. The results from the experiments with pure wood pellet (Part B) showed only a few µm thick oxide layers (0-6 µm) at all steel ring temperatures (450 °C – 550 °C). Also, when firing doped wood pellets (Part A) at 450 °C the oxide layer was quite thin (3-7 µm). The corrosion increased, however, with increasing temperature, and the thickest oxide layer was measured at 10CrMo9-10 when the ring temperature was set to 550 °C (> 70 µm at 45°). The overall difference in the oxide layer growth while burning pure and doped wood pellet is easy to notice and the contribution of Zn and Cl in the corrosion process is quite clear. The corrosion of low-alloy steel when combusting a Zn and Cl containing fuel may be substantial compared to a pure biomass fuel.

From the EDX analyses of the 10CrMo9-10 cross-sections it can be assumed, based on the atomic ratios, that hematite (Fe_2O_3) together with magnetite (Fe_3O_4) formed layered corrosion products on the steel. Closer to the scale/flue gas interphase, an enrichment of KCl was observed. In some cases, the molar amount of Cl found on the top of the oxide scale was more than twice the amount of K. Zn was also present. The atomic ratio of Cl/K/Zn implied the presence of K_2ZnCl_4, together with some ZnO. This is in agreement with Robelin and Chartrand [117], who showed that the formation of a K_2ZnCl_4 phase is possible in KCl-$ZnCl_2$ mixtures. The surface of the 10CrMo9-10 steel after the combustion test with doped fuel was Cl-rich and cracked. The cracks were filled with $FeCl_2$ (Figure 22). The low ash input (around 130 g/test with doped fuel) and short probe exposure times (7 h) resulted in a low rate of deposit buildup (RBU) in all cases. The maximum RBU was 20 g m^{-2} h^{-1}. The EDX analysis

of the windward side deposit showed enrichment in ZnO, which was the main compound, elevated amounts of KCl, and small amounts of Ca and S. The leeward side contained additionally small amounts of SiO_2, Al_2O_3, and MgO.

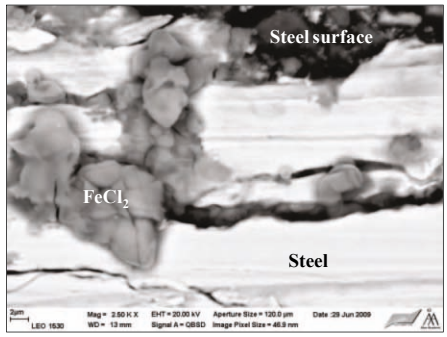

Figure 22. BSE-SEM image of the cross-section of the 10CrMo9-10 steel ring after 7 h with doped fuel and a test ring temperature of 450 °C (Paper IV).

4.3 Waterwall corrosion & determination of the corrosive species during co-firing of SRF

In waste-fired boilers, high-temperature corrosion has usually been attributed to the presence of chlorides, which together with Zn and Pb form mixtures that melt at relatively low temperatures [20, 22]. Additionally, the issue of high-temperature corrosion induced by bromides has been raised lately [10].

In the Anjalankoski BFB boiler a significant corrosion in the lower furnace on the front and back waterwalls was observed. Both Cl and Br were found on the corrosion front. The waterwall temperature was estimated to be around 400 °C. At these temperatures Zn and Pb chlorides play a more important role in the corrosion of boiler tube materials than alkali (K, Na) chlorides. To shed more light on the reasons for such corrosion, and also to clarify the occurrence of Cl, Br, Zn and Pb in the furnace vapours and in the deposit on the boiler waterwalls, a measurement campaign was undertaken (**Papers V & VI**). To support and evaluate the findings, a thermodynamic equilibrium analysis was also made. The thermodynamic calculations helped to interpret in which forms the ash forming elements were both in the combustion gases and in the deposits of the examined boiler. Laboratory tests were also carried out to estimate the degree of corrosion of boiler steels under bromine and zinc containing deposits. Since both chlorides and bromides were found to be corrosive, the tests were also focused to determine their relative corrosiveness. The laboratory test results are part of *Section 4.1*.

4.3.1 Vapours and gas composition

Figure 23 shows the concentrations of the water-soluble elements in the fine particle matter as sampled from the combustion gases next to the left waterwall (neighbouring wall on the level of the corroded areas). It was determined that approximately 40% of Pb, 50% of Zn and 35% of Cu formed water soluble compounds. The corresponding numbers for Na and K were 80% and 100%, respectively. Based on the analyses it was estimated that roughly 80% of the fine

mode particles were composed of the elements mentioned above. The formation of sulphates was negligible and the amount of sulphate anion was 1-2 ppm. The measurements on the front wall showed that the concentration of fine particles was half of that measured on the left wall.

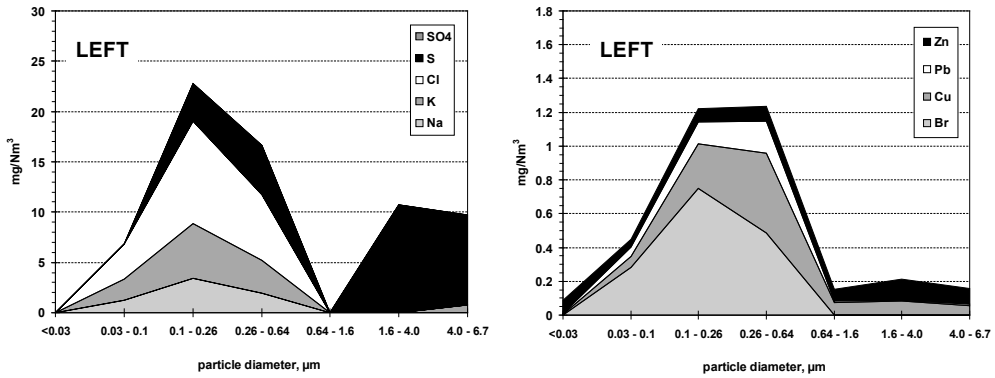

Figure 23. Concentration of fine particle forming matter in the combustion gases next to the left wall, based on water soluble wet chemical analyses. SO_4 denotes the amount of sulfur in the form of sulphate calculated as elemental sulfur, while S denotes elemental sulfur in a form other than sulphate (Paper V).

The concentrations of both Cl and Br correlated positively with the concentration of the Zn + Pb + Cu. The atomic ratios showed that Zn, Pb, and Cu were able to bind approximately 10% of the halogens. The rest are Na and K halides that were able to bind >85% of the halogens. It was also an indication of a negligible formation of sulphates.

The gas analyses next to the front and the left wall showed that the walls were exposed to conditions which were fluctuating in between oxidizing and reducing. The gas composition was also changing. The GC analysis applied to the measurements on the left wall showed that some 75% of of the gaseous S was present as SO_2 and rest as H_2S. It was also shown that the conditions at the front wall were predominantly oxidising while at the left wall they were predominantly reducing.

4.3.2 Deposits

The analyses of the deposit samples from both corroding walls (front and back) showed no significant differences between the walls. Substantial differences in the compositions were, however, observed along the wall heights. The deposits from the lower parts of both walls (levels F1-F3, Figure 24) were rich in alkali chlorides (KCl, NaCl) along with smaller amounts of Br. Bromine was found frequently in combination with K and/or Na and thus it was most likely present as KBr and/or NaBr (Figure 25). The deposit from the higher levels (not corroding) composed almost entirely of K-, Na- and Ca- sulphates while the amounts of Cl and Br were negligible.

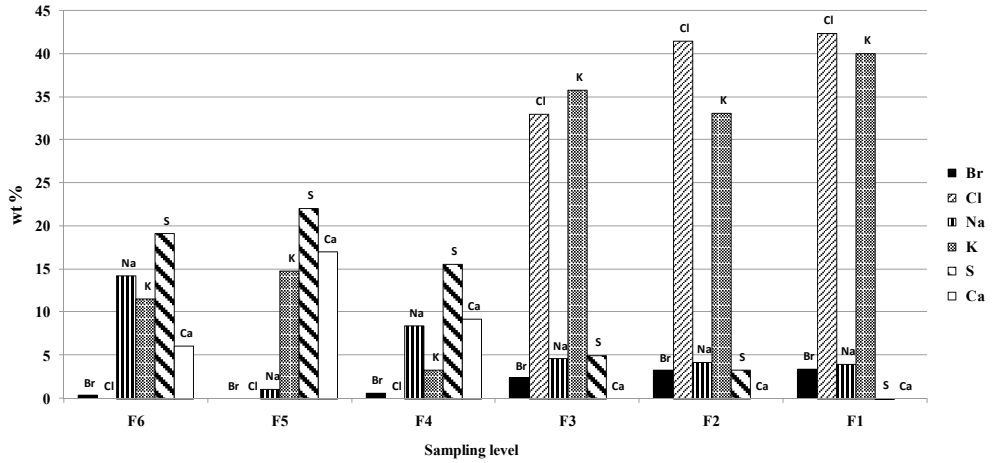

Figure 24. Concentrations of most abundant elements in the waterwall deposits sampled from different levels of the front wall.

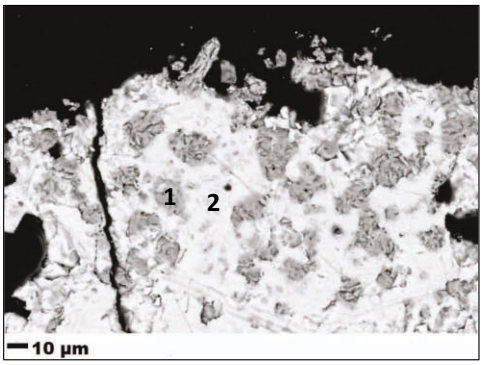

Wt.%	1	2
O	43.88	9.7
Na	0.18	4.02
S	22.33	0.17
Cl	0.44	44.66
K	15.51	38.17
Ca	17.34	-
Br	0.04	3.07

Figure 25. BSE-SEM image of the cross-section of a deposit sampled from the bottom part of the heavily corroded area of the back wall and the results of the EDX point analysis (Paper V).

Zn, Pb as well as some Cu were identified locally. Zn and Cu were often found together with S and/or Cl. Based on the atomic ratios it was concluded that they were in the form of sulphates and, very occasionally as chlorides. Spot analyses of Pb precipitates showed enrichment of Cl indicating the presence of $PbCl_2$, especially in the deposit sampled from the corroded part of the front wall (Figure 26). The presence of $PbCl_2$ in the deposit may significantly increase the corrosion as shown in Papers I & III. Pb was also found in the deposit on the waterwalls where corrosion did not occur, but Cl was not present.

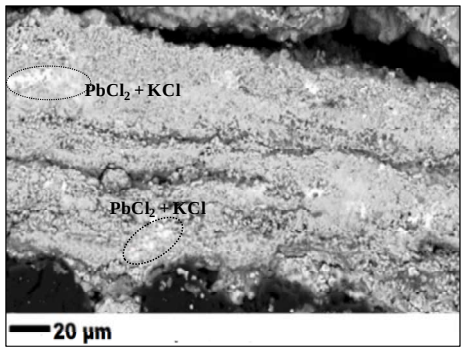

Figure 26. BSE-SEM image of the cross-section of the deposit sampled from the bottom part of the heavily corroded area of the front wall (Paper V).

4.3.3 Thermodynamic equilibrium calculations

Thermodynamic calculations were performed to predict the chemical forms of the ash forming elements in the combustion gases and in the waterwall deposits in the examined boiler with focus on Zn. Pb, Cl and Br.

Figure 27 shows the predicted forms of Zn and Pb at 1100 °C and 400 °C in reducing and oxidising conditions. At 1100 °C, Pb is present in gaseous Pb(g) and PbS(g) at reducing and as PbO(g) at oxidising conditions , while the analysis of the deposit indicated the presence of $PbCl_2$. This was the only discrepancy found between the modelled deposit composition and the analysed composition concerned the Pb, and it suggests that local conditions were different from the conditions considered in the modelling. Zinc seems to be present in the form of Zn(g) at reducing conditions and as a solid silicate at oxidising conditions with a minor fraction being gaseous $ZnCl_2$(g). In the vapours sampled from the boiler, approximately half of the Zn and Pb were found to be water soluble. This finding partially supports, the modelled speciation of Zn of which some part was estimated to be present also as $ZnCl_2$(g).

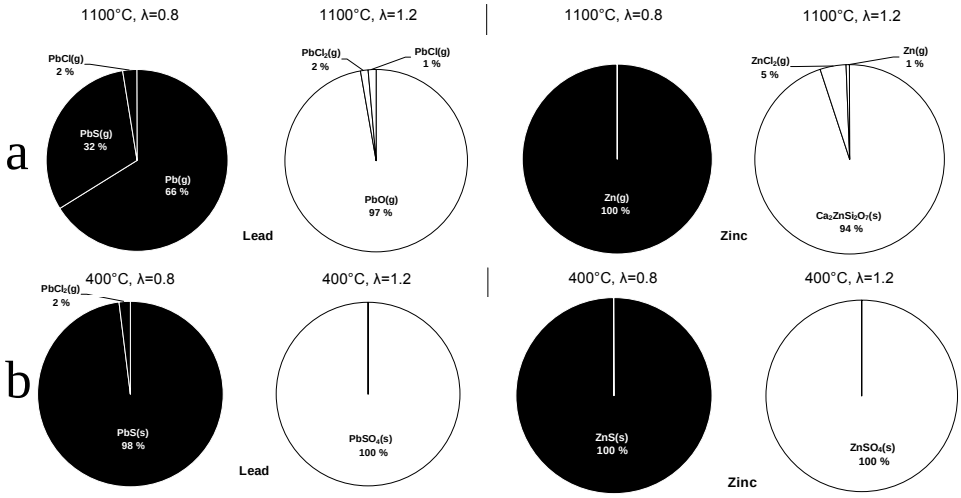

Figure 27. The predicted forms of a) Pb and Zn at 1100 °C and b) Pb and Zn at 400 °C in reducing (black) and oxidising (white) conditions in BFB boiler firing SRF. The proportions with less than 1% are excluded from the charts (Paper VI).

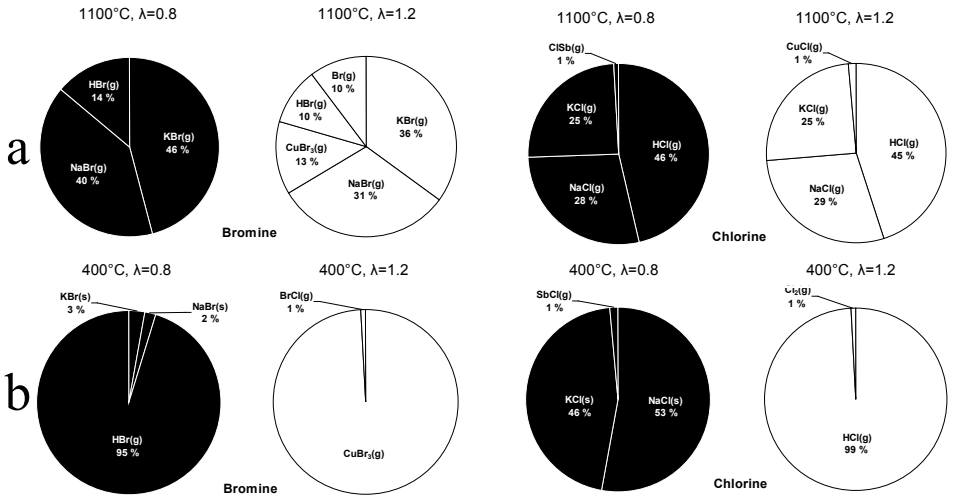

Figure 28. The predicted forms of a) Br and Cl at 1100 °C and b) Br and Cl at and 400 °C in reducing (black) and oxidising (white) conditions in BFB boiler firing SRF. The proportions with less than 1% are excluded from the charts (Paper VI).

At 400 °C, the forms of the Pb and Zn were very similar to each other. They form solid sulphides and sulphates under reducing and oxidising conditions, respectively. This agrees with the findings that Zn in the deposit was present as sulphate, but the presence of ZnS, however, cannot be excluded.

Figure 28 shows the predicted forms of Br and Cl in both combustion gases (at 1100 °C) and in the deposits (at 400 °C) in reducing and oxidising conditions. At 1100 °C, Br is present in oxidising and reducing conditions mainly as gaseous NaBr, KBr, with smaller amounts of other Br-compounds such as HBr, $CuBr_3$ and Br. The predicted forms of Cl were, apart from HCl, mainly gaseous NaCl and KCl. At the deposit temperature (400 °C) in reducing conditions Br seems to be present to a high extent as HBr but also as solid KBr and NaBr. In oxidising conditions roughly 99% of Br is present as gaseous $CuBr_3$. In reducing conditions Cl is expected to be present as alkali chlorides (NaCl and KCl) and almost entirely as HCl in oxidising conditions. The predicted forms are in agreement with the analysis of the deposit samples. The deposit composed of mainly of KCl and NaCl along with small amounts of KBr.

5. CONCLUSIONS

The combustion of waste-derived fuels creates an aggressive combustion atmosphere due to the presence of chlorides and heavy metals, particularly of Zn and Pb. The research showed that chlorides of these metals may significantly decrease the first melting temperature of a deposit and also influence on the amount of melt in the deposit, which in turn may accelerate corrosion of the boiler's heat exchanging materials. However, in some cases it was found that the presence of melt was not necessary to cause severe corrosion. It was also shown that apart from the presence of chlorides also bromides may cause corrosion. At low material temperatures bromides were shown to be more corrosive than chlorides.

The corrosiveness of different Zn- and Pb- compounds both as single salts and in mixtures was investigated in the laboratory (*Papers I-III*). It was shown that $PbCl_2$ caused severe corrosion on the two test materials (10CrMo9-10 and AISI 347) already below the melting temperature of $PbCl_2$, showing that the presence of melt in the case with $PbCl_2$ was not necessary to cause severe corrosion. The $PbCl_2$, was aggressive to the low-alloy (10CrMo9-10) and also to the stainless steel (AISI 347) at temperatures above 350 °C. The poor resistance of AISI 347 was ascribed to $PbCrO_4$ formation that significantly decreased the protectiveness of Cr_2O_3.

The $PbCl_2$-containing mixtures: $PbCl_2$-K_2SO_4, $PbCl_2$-KCl and $PbCl_2$-$ZnCl_2$-KCl caused significant corrosion to the low-alloy steel (10CrMo9-10) at 400 °C and to AISI 347 at 500 °C and above. The highest corrosion at 400 °C was observed when both $PbCl_2$ and $ZnCl_2$ were present. The $PbCl_2$-$ZnCl_2$-KCl mixture contained the highest fraction of melt out of all tested salt mixtures but the corrosiveness of this mixture was not the highest at all test temperatures. Accordingly, the amount of melt does not necessarily decide the corrosion level. At 500 °C and above, the corrosion caused by all three mixtures containing $PbCl_2$ was extreme and similar on both materials. The results from the tests with the mixtures containing 5 wt-% $PbCl_2$ were similar to the results from the tests with pure $PbCl_2$, showing its highly corrosive character.

The exposures to $ZnCl_2$ showed negligible oxide layer growth on AISI 347 in the temperature range of 250-450 °C. The good resistance of AISI 347 was attributed to the protective Cr_2O_3. The Cr_2O_3 did not form Zn-chromate thus its integrity was not destroyed. However, the low-alloy steel 10CrMo9-10 suffered from an increased oxide layer growth already at 350 °C by formation of $ZnFe_2O_4$ and $FeCl_2$. Above 350 °C, the oxide layer growth was suppressed due to the fast evaporation of $ZnCl_2$ with increasing temperature. In the tests with $ZnCl_2$ the harmful influence of the presence of a melt was more obvious. The extent of corrosion increased drastically when the test temperature was above the $ZnCl_2$ melting temperature of 318 °C.

The $ZnCl_2$-containing mixture ($ZnCl_2$-$PbCl_2$-KCl) was shown to be more aggressive and active at lower temperatures than $PbCl_2$-KCl. It suggests that $ZnCl_2$ is thus more likely to cause problems at lower material temperatures (waterwall/economiser). While $PbCl_2$ is less volatile and, therefore, may be present in the deposit also at higher temperatures, it is expected that $PbCl_2$ is most likely to be problematic at both waterwall and superheater temperatures.

The exposures to Zn- and Pb-oxides at 550 °C showed that ZnO is neither corrosive to the low-alloy steel (10CrMo9-10) nor to the stainless steel (AISI 347). The oxide layer thickness was comparable to the test in which there was no salt present. The exposures of low-alloy steel to PbO resulted in a noticeable oxide layer. The oxide layer on the stainless steel was low and $PbCrO_4$ was identified as one of the corrosion products.

The tests performed in a bench scale fluidized bed reactor firing wood pellets doped with $ZnCl_2$ (*Paper IV*) confirmed the laboratory test results and showed that the presence of $ZnCl_2$ has a readily noticeable impact on high-temperature corrosion of low-alloy steel. When comparing to combustion of pure wood pellet, the corrosion was enhanced above 450 °C. The

probe deposit was rich in K_2ZnCl_4 which was attributed to be the direct cause of corrosion. The high-alloy steel (S28) showed a good resistance.

A full scale measurement campaign in an SRF fired bubbling fluidised bed boiler (*Papers V and VI*) showed that the deposit from the corroded waterwall and that the ash forming vapours in the furnace was enriched with Cl and little Br but also with Zn and Pb. Chemical thermodynamic calculations indicated that Zn and Pb were present mainly as solid sulphides or sulphates in reducing and oxidizing conditions, respectively, while Cl and Br most likely formed alkali bromides and chlorides. The thermodynamic calculations were in correlation with the deposit analysis. The fluctuating conditions and a deposit rich in alkali chlorides and alkali bromides and some $PbCl_2$ was shown to cause serious corrosion in the SRF fired boiler. Laboratory tests were also carried out to estimate the degree of corrosion of boiler steels under bromine containing deposits. The $ZnBr_2$-K_2SO_4 salt mixture was tested in air and in a reducing atmosphere and the results were compared with the tests with $ZnCl_2$-K_2SO_4. The mixture with $ZnBr_2$ was found to be more aggressive at 400 °C in oxidising conditions than the corresponding mixture with $ZnCl_2$. The oxide layer formed on non-alloy (St 45.8/III) and low-alloy (10CrMo9-10) steels was low at 350 °C (5 and 10 µm, respectively) and a bit higher but still quite low at 400 °C (~15 µm). The AISI 347 and S28 did not show any detectable corrosion. The results indicate that 350 °C may be a safe level for waterwall temperature when the deposit contains some $ZnBr_2$ in both oxidising and reducing conditions. Above 350 °C, transformation of $ZnBr_2$ to KBr was observed.

In general it can be concluded that lead compounds, $PbCl_2$ and PbO, are quite corrosive if they deposit on tubes or walls with surface temperatures over 350 °C in the case of $PbCl_2$. To avoid Pb-induced corrosion may be difficult. One way could be to try to transform the corrosive compounds to $PbSO_4$, since sulphates are known to be less corrosive than chlorides. However, the corrosiveness of $PbSO_4$ has not been investigated in this work, and it is not well known how the compound behaves on metals. Another way would be to separate the Pb-containing objects before combustion.

Also $ZnCl_2$ was found to be corrosive at fairly low temperatures (350 °C), while ZnO did not cause any severe corrosion. Since the stable forms of Zn in combustion is ZnO and/or $ZnSO_4$, the risk of Zn-induced corrosion is small as it was shown that ZnO is not corrosive. $ZnSO_4$ was not tested but as mentioned above sulphates are less corrosive than chlorides. Nevertheless, $ZnCl_2$, if it is introduced as such into the combustion process, may cause corrosion if there is not enough time and/or oxygen to oxidise it to ZnO before deposition.

Future work

The results obtained within this work showed that Zn- and Pb-containing compounds cause serious corrosion of boiler tube materials in waste-fired boilers in different temperature ranges and to different extents on different materials. It is of considerable importance that there are further studies investigating the corrosiveness of such compounds in the presence of gaseous species present in waste-fired boilers and in relation to different materials. In addition, the newly discovered but as yet not investigated problem of Br-induced corrosion requires further work.

REFERENCES

[1] Manders J. ISWA/Dakofa conference 3rd December 2009, Copenhagen, Denmark http://www.cewep.eu/storage/med/media/energy/283_Renew_Energy_Europe__JM_7.pdf (accessed 10, February 2012).

[2] Krause H. H. *Chlorine Corrosion in Waste Incineration*. The European Corrosion Congress EUROCORR 97'. Trondheim, Norway (1997) Conference Proceedings.

[3] Meisen P., Phipps-Morgan I. *Waste-to-Energy Plants*. Global Energy Network Institute GENI (2010).

[4] Directive 2000/76/EC of the European Parliament and of the Council of 4 December 2000 on the incineration of waste. Official Journal of the European Communities, 28.12.2000.

[5] Directive 2008/98/EC of the European Parliament and of the Council of 19 November 2008 on waste and repealing certain Directives. Official Journal of the European Union, 22.11.2008.

[6] Directive 2009/28/EC of the European Parliament and of the Council of 23 April 2009 on the promotion of the use of energy from renewable sources and amending and subsequently repealing Directives 2001/77/EC and 2003/30/EC. Official Journal of European Union, 5.6.2009.

[7] Viklund P. *High-temperature corrosion during waste incineration. Characterization, causes and prevention of chlorine-induced corrosion.* Licentiate Thesis, Kungliga Tekniska Högskolan, Stockholm, Sweden, (2011).

[8] Lee S-H., Themelis N. J., Castaldi M. J. *High-Temperature Corrosion in waste-to-Energy Boilers.* J Therm Spray Technol 16 (2007) 104-110.

[9] Pedersen A. J., Frandsen F. J., Riber C., Astrup T., Thomsen S. N., Lundtorp K, Mortensen L. F. *A Full-scale Study on the Partitioning of Trace Elements in Municipal Solid Waste Incineration-Effects of Firing Different Waste Types.* Energy Fuel 23 (2009) 3475-3489.

[10] Vainikka P., Enestam S., Silvennoinen J., Taipale R., Yrjas P., Frantsi A., Hannula J., Hupa M. *Bromine as an ash forming element in a fluidised bed boiler combusting solid recovered fuel.* Fuel 90 (2011) 1101–1112.

[11] Becidan M., Sørum L., Frandsen F., Pedersen A. J. *Corrosion in waste-fired boilers: A thermodynamic study*. Fuel 88 (2009) 595-604.

[12] Talonen T. *Chemical Equilibria of Heavy Metals in Waste Incineration: Comparison of Thermodynamic Databases.* Lic. Thesis. Åbo Akademi University, Finland (2008).

[13] Zhang Y-L., Kasai E. *Effect of Chlorine on the Vaporization Behavior of Zinc and Lead during High temperature treatment of Dust and Fly Ash.* ISIJ Int., Vol. 44 , No. 9, (2004) 1457-1468.

[14] Bøjer M., Jensen P. A., Frandsen F., Dam-Johansen K., Madsen O. H., Lundtorp K. *Alkali/Chloride release during refuse incineration on a grate: Full-scale experimental findings.* Fuel Process Technol 89 (2008) 528-539.

[15] Osad S., Kuchar D., Matsuda H. *Effect of chlorine on volatilization of na, K, Pb and Zn compounds from municipal solid waste during gasification and melting in a shaft-type furnace.* J Mater Cycles Waste Manage 11 (2009) 367-375.

[16] Chan C., Jia C., Graydon J. W., Kirk D. W. *The bahaviour of selected heavy metals in MSW incineration electrostatic precipitator ash during roasting with chlorination agents.* J Hazard Mater 50 (1996) 1-13.

[17] Spiegel M. *Salt melt induced corrosion of metallic materials in waste incineration plants.* Mater Corros 50 (1999) 373-393.

[18] Otsuka N. *A thermodynamic approach on vapor-condensation of corrosive salts from flue gas on boiler tubes in waste incinerators.* Corros Sci 50 (2008) 1627–1636.

[19] Waltl J., Rechberger N. *The task of chemistry in biomass plants applied in the Timelkam Power Plant.* VGB PowerTech 3 (2006) 48-52.

[20] Norell M., Andersson P. *Field test of waterwall corrosion in a CFB waste boiler.* CORROSION 2000, March 26–31. Orlando, FI: NACE International (2000).

[21] Skrifvars B.-J., Backman R., Hupa M., Salmenoja K., Vakkilainen E. *Corrosion of superheater steel materials under alkali salt deposits Part1: The effect of salt deposit composition and temperature.* Corros Sci 50 (2008) 1274-1282.

[22] Sánchez-Pastén M., Spiegel M. *High-temperature corrosion of metallic materials in simulated waste incineration environments at 300–600 °C.* Mater Corros 57 (2006) 192–195.

[23] Fukusumi M., Okanda Y. *High-temperature corrosion in Municipal Waste Incineration-Influence of Combustion Ashes.* Symposium on "High-Temperature Materials Problems in Waste Incineration Systems", Corrosion 87/89, NACE Publications.

[24] Krause H. H. *Chlorine Corrosion in Waste Incineration.* Symposium on "High-Temperature Materials Problems in Waste Incineration Systems", Corrosion 87/89, NACE Publications.

[25] Enestam S. *Corrosivity of hot flue gases in the fluidized bed combustion of recovered waste wood*. Academic Dissertation , Åbo Akademi, Faculty of Chemical Engineering, Process Chemistry Centre, Åbo, Finland (2011).

[26] Weinzierl K., Äijälä M., Sandin O.O., Luxhoi F., Doets N., Jaud P., Lemmens N. D., Mendez de Vigo I., Dodero G., Almiro R., Heinonen O. *Power production from biomass – Thermal generation study committee.* Union of the Electric Industry – EURELECTRIC. Brussels, Belgium (1997), www.eurelectric.org/Download/Download.aspx?DocumentID=5593 (accessed on March 15, 2012).

[27] Howard J. R. *Fluidized Beds – Combustion and Applications.* Applied Science Publishers (1983).

[28] Oka S. N. *Fluidized Bed Combustion*. Marcel Dekker, Inc. New York, USA (2004) ISBN: 0-8247-4699-6.

[29] Basu P. *Combustion and Gasification in Fluidized Beds.* Taylor and Francis Group, LLC. (2006) ISBN 0-8493-3396-2.

[30] High-alloy Materials for Boiler Tubes. Salzgitter Mannesmann Stainless Tubes. http://www.smst-tubes.com/fileadmin/media/pdf_broschueren/SMST-Tubes_Boiler_Brochure_2009.pdf (accessed on March 18, 2012).

[31] Talbot D. E. J., Talbot J. D. R. *Corrosion Science and Technology 2nd Edition.* CRC Press, Taylor & Francis Group (2007) ISBN: 0-8493-9248-9.

[32] Khanna A. S. *Introduction to High Temperature Oxidation and Corrosion.* ASM International (2002) ISBN: 0-87170-762-4.

[33] Evans U. R. *An Introduction to Metallic Corrosion* 3rd Edition. Edward Arnold Ltd. (1981) ISBN 0-7131-2758-9.

[34] Lai G. Y. *High-temperature corrosion of Engineering Alloys.* ASM International (1990) ISBN: 0-87170-411-0.

[35] Schweitzer P. A. *Fundamentals of Metallic Corrosion. Corrosion Engineering Handbook* 2nd Edition. CRC Press, Taylor & Francis Group (2007) ISBN: 0-8493-8243-2.

[36] *Sandvik Sanicro 28, Composite tubes for steam boiler applications.* http://www.smt.sandvik.com/Global/Downloads/Products_downloads/tubular-products/S-12111-ENG%20050822.SAN28%20pdf.pdf (accessed on March 26, 2012).

[37] Noguchi M., Yakuwa H., Miyasaka M., Yokono M., Matsumoto A., Miyoshi K., et al. *Experience of superheater tubes in municipal waste incineration plant.* Mater Corros 51 (2000) 774–785.

[38] European Cooperation in Science and Technology (COST). COST Action E31: *Management of Recovered Wood*; COST: Brussels, Belgium (2007), http://www.ctib tchn.be/coste31/frames/f_e31.htm (accessed on July 6, 2010).

[39] Swedish Energy Agency. *Trädbränsle- och trovpriser.* Nr 3/2011; http://webbshop.cm.se/System/TemplateView.aspx?p=Energimyndigheten&view=default &id=3206cbb3952c4e6088cbd1f297503c16 (accessed on November 22, 2011).

[40] Krook J., Mårtensson A., Eklund M. *Sources of heavy metal contamination in Swedish wood waste used for combustion.* Waste Manage 26 (2006) 158–166.

[41] Maine Energy Systems, LLC (MESys). *Systems Wood Pellets—Basic Training*. MESYS: Bethel, Maine, 2007; http://www.maineenergysystems.com/userfiles/files/Wood%20the%20renewable%20energy%20Source. pdf (accessed on June 6, 2010).

[42] Vainikka P. *Occurrence of bromine in fluidised bed combustion of solid recovered fuel.* Academic Dissertation, Åbo Akademi, Faculty of Chemical Engineering, Process Chemistry Centre, Åbo, Finland (2011).

[43] CEWEP Brochure. *Heating and Lighting the Way to a Sustainable Future*. (2010) http://www.cewep.eu/ information/publicationsandstudies/statements/ceweppublications/index.html (accessed on November 10, 2011).

[44] Schrör H. *Generation and treatment of waste in Europe 2008 – Steady reduction in waste going to landfills.* EUROSTAT statistics in focus 44 (2011) http://epp.eurostat.ec.europa.eu/cache/ITY_OFFPUB/KS-SF-11-044/EN/KS-SF-11-044-EN.PDF (accessed on November 14, 2011).

[45] The European Committee for Standardization (CEN). CEN/TC 343. Solid recovered fuels (2010).

[46] van Tubergen J., Glorius T., Waeyenbergh E. *Classification of Solid Recovered Fuels.* European Recovered Fuel Organisation (2005) Download: www.erfo.info, www.erfo.eu (accessed February 7, 2012).

[47] Rotter V. S., Kost T., Winkler J., Bilitewski B. *Material flow analysis of RDF-production processes.* Waste Manage 24 (2004) 1005-1021.

[48] Gendebien A., Leavens A., Blackmore K., Godley A., Lewin K., Whiting K.J., Davis R., Giegrich J., Fehrenbach H., Gromke U., del Bufalo N., Hogg D. *Refuse Derived Fuel, Current Practice and Perspectives* (B4-3040/2000/306517/MAR/E3). European Commission – Directorate General Environment, Report No.: CO 5087-4 (July, 2003).

[49] Scoullos M., Siskos P., Zeri C., Skordilis A., Ziogas Ch., Sakellari A., Giannopoulou K., Tsiolis P., Mavroudeas S., Argyropoulos I., Roumeliotis Th., Skiadi O. *Composition and Chemical Properties of RDF Produced at a MSW Mechanical Separation Plant in Greece*. (2009).

[50] Tolcin A. C., *Minerals yearbook, metals & minerals–zinc*. USGS (2007).

[51] Lalykin N., Mikhaleva O., Kulapina E., Eremenko S. *Separate identification of copper (II) and zinc (II) in tinted crystal glass.* Glass Ceram 61 (2004) 221–223.

[52] Zweifel H. *Plastics additives handbook.* 5th edition Cincinnati, OH: Hanser Gardner Publications (2000).

[53] Krook J.; Mårtensson A.; Eklund M. *Metal contamination in recovered waste wood used as energy source in Sweden.* Resour Conserv Recycl 41 (2004) 1–14.

[54] Vainikka P., Bankiewicz D., Frantsi A., Silvennoinen J., Hannula J., Yrjas P., Hupa M. *High-temperature corrosion of boiler waterwalls induced by chlorides and bromides. Part 1: Occurrence of the corrosive ash forming elements in a fluidised bed boiler co-firing solid recovered fuel.* Fuel 90 (2011) 2055-2063.

[55] Frandsen F., Pedersen A.-J., Hansen J., Madsen O.-H., Lundtorp K., Mortensen L. *Deposit formation in the FASAN WtE boiler as a function of feedstock composition and boiler operation.* Energy Fuels 23 (2009) 3490–3496.

[56] Nakamura K., Kinoshita S., Takatsuki H. *The origin and behavior of lead. Cadmium and antimony in MSW incinerator.* Waste Manage 16 (1996) 509–517.

[57] Wenchao M., Rotter S. *Overview on the chlorine origin of MSW and Cl-originated corrosion during MSW & RDF combustion process.* The 2nd international conference on bioinformatics and biomedical engineering. Shanghai, China, ICBBE (2008).

[58] Alaee M., Arias P., Sjödin A., Bergman Å. *An overview of commercially used brominated flame retardants, their applications, their use patterns in different countries/regions and possible modes of release.* Environ Int 29 (2003) 683–689.

[59] Wiik C. *Pre-normative research on solid solid biofuels for improved European standards* BioNorm II–Project no. 038644. (2008) http://www.bionorm2.eu/mo-files/downloads/DIV.6%20part2%20used%20wood%20classification.pdf (accessed November 11, 2011).

[60] Werkelin J. *Ash-forming elements and their chemical forms in woody biomass fuels.* Academic Dissertation , Åbo Akademi, Faculty of Chemical Engineering, Process Chemistry Centre, Åbo, Finland (2008).

[61] Vainikka P., Silvennoinen J., Yrjas P., Frantsi A., Hietanen L., Hupa M., et al. *Bromine and chlorine in aerosols and fly ash when co-firing solid recovered fuel, spruce bark and paper mill sludge in 80MWth BFB boiler*. The 20th international conference on fluidized bed combustion, Xian, China (2009).

[62] van Esch G., J. *Flame retardants: a general introduction*. Geneva: World Health Organization (1997).

[63] Niemi J. *The influence of lead and zinc on deposit formation in fluidized bed combustion of demolition wood.* MSc thesis, Åbo Akademi, Faculty of Chemical Engineering, Process Chemistry Centre, Åbo, Finland (2006).

[64] Åmand L., Leckner B., Eskilsson D., Tullin C. *Ash deposition on heat transfer tubes during combustion of demolition wood.* Energy Fuels 20 (2006) 1001–1007.

[65] Elled A., Åmand L., Eskilsson D. *Fate of zinc during combustion of demolition wood in a fluidized bed boiler.* Energy Fuels 22 (2008) 1519–1526.

[66] Forsberg C. *BFB furnace bottom modification in Idbäcken CHP*. Second international conference on biomass and waste combustion. Oslo, Norway (2010) Conference Proceedings.

[67] Wright I. G., Krause H. H. *Assessment of factors affecting boiler tube lifetime in waste-fired steam generators: new opportunities for research and technology development.* New York: ASME (1996).

[68] Daniel P. L., Barna J. L., Blue J. D. *Furnace-Wall Corrosion in Refuse-Fired Boilers.* (1986).

[69] Kautz K. M. *The Causes of Boiler Metal Wastage in the Standtwerke Dusseldorf Incineration Plant.* Proceedings of the symposium High-temperature corrosion in Energy Systems. A publication of the Metallurgical Society of AIME (1985).

[70] Rademakers P., Hesseling H., van De Wetering J. *Review on corrosion in waste incinerators and possible effect of bromine.* TNO Industrial Technology, TNO report I02/01333/RAD, Apeldoorn, Netherlands (2002).

[71] Kerekes Z. E., Bryers R. W., Sauer A. R. *The Influence of Heavy Metals Pb and Zn on Corrosion and Deposits in Refuse-Fired Steam Generators,* (1985).

[72] Daniel P. L., Paul L. D., Barna J. *Fire-side Corrosion in Refuse-fired Boilers.* Symposium on "High-Temperature Materials Problems in Waste Incineration Systems", Corrosion 87/89, NACE Publications.

[73] Miller P. D., Krause H. H. *Metal Corrosion in Incinerators.* Solid Waste Treatment 122, vol. 68 (1971) AIChE Symposium Series.

[74] Noguchi M., Yakuwa H., Miyasaka M., Yokono M., Matsumoto A., Miyoshi K., et al. *Experience of superheater tubes in municipal waste incineration plant.* Mater Corros 51 (2000) 774–785.

[75] Nielsen H. P., Frandsen F. J., Dam-Johansen K. *Lab-scale Investigations of High-Temperature Corrosion Phenomena in Straw-Fired Boilers.* Energy Fuels 13 (1999) 1114-1121.

[76] Frandsen F. J. *Utilizing biomass and waste for power production - a decade of contributing to the understanding, interpretation and analysis of deposits and corrosion products.* Fuel 84 (2005) 1277-1294.

[77] Nielsen H. P., Frandsen F. J., Dam-Johansen K., Baxter L. L. *The implications of chlorine-associated corrosion on the operation of biomass-fired boilers.* Prog Energ Combust 26 (2006) 283-298.

[78] Salmenoja K. *Field and Laboratory Studies on Chlorine-induced Superheater Corrosion in Boilers Fired with Biofuels*. Academic Dissertation, Åbo Akademi, Faculty of Chemical Engineering, Process Chemistry Centre, Åbo, Finland (2000).

[79] Grabke H. J., Reese E., Spiegel M. The effects of chlorides, hydrogen chloride, and sulfur dioxide in the oxidation of steels below deposits. Corros Sci 37 (1995) 1023-1043.

[80] Gotthaelp K., Brønsted P., Jansen P., Markussen J., Montgomery M., Maahn E. *High-temperature corrosion In Biomass Incineration Plants.* Final Report: EFP95 Project no. 1323/95-0008(1997).

[81] McNallan M. J., Liang W. W., Kim S. H., Kang C. T. *Acceleration of the High Temperature Oxidation of Metals by Chlorine.* High-temperature corrosion. NACE, Houston, Texas (1983) 316-321.

[82] Salmenoja K., Hupa M., Backman R. *Laboratory studies on the influence of gaseous HCl on superheater corrosion.* Impact of Mineral Impurities in Solid Fuel Combustion, edited by Gupta et al. Kluwer Academic/Plenum Publishers, New York (1999).

[83] Hiramatsu N., Uematsu Y., Tanaka T., Kinugasa M. *Effects of Alloying Elements on NaCl-induced Hot Corrosion of Stainless Steels.* Mater Sci Eng, A120 (1989) 319-328.

[84] Pettersson C., Pettersson J., Asteman H., Svensson J.-E., Johansson L.-G. *KCl-induced high-temperature corrosion of the austenitic Fe-Cr-Ni alloys 304L and Sanicro 28 at 600 °C.* Corros Sci 48 (2006) 1368-1378.

[85] Hupa M., Backman P., Backman R., Tran H. *Reactions Between Iron and HCl-Bearing Gases in Incinerating municipal and industrial waste.* Bryers RW, New York, Hemisphere (1989) p. 191.

[86] Backman R., Hupa M., Hiltunen M., Peltola K. *Interaction of the Behaviour of Lead and Zinc with Alkalis in Fluidized Bed Combustion or Gasification of Waste Derived Fuels.* 18th International Conference on Fluidized Bed Combustion, May 22-25, 2005 Toronto, Canada, Conference Proceedings.

[87] Krause H. H., Vaughan D. A., Miller P. D. *Corrosion and Deposits From Combustion of Solid Waste.* J Eng P (1973) 45-52.

[88] Spiegel M. *Influence of gas phase composition on the Hot Corrosion of steels and nickel-based alloys beneath a (Ca-Na-K)-sulfate mixture containing $PbSO_4$ and $ZnSO_4$.* Mater Corros 51 (2000) 303-312.

[89] Li Y. S, Niu Y., Wu W. T. *Accelerated corrosion of pure Fe, Ni, Cr and several Fe-based alloys induced by $ZnCl_2$-KCl at 450 ºC in oxidizing environment*. Mater Sci Eng, A 345 (2003) 64-71.

[90] Li Y. S., Spiegel M. *Models describing the degradation of FeAl and NiAl alloys induced by $ZnCl_2$-KCl melt at 400-450 ºC.* Corros Sci 46 (2004) 2009-2023.

[91] Pan T. J., Zeng C. L., Niu Y. *Corrosion of Three Commercial Steels Under $ZnCl_2$-KCl Deposits in a Reducing Atmosphere Containing HCl and H_2S at 400-500 ºC.* Oxid Met 67 (2007).

[92] Lu W. M., Pan T. J., Zeng C. L., Niu Y. *Accelerated corrosion of five commercial steels under a $ZnCl_2$-KCl deposit in a reducing environment typical of waste gasification at 673-773 K.* Corros Sci 50 (2008) 1900-1906.

[93] Li Y. S., Al-Omary M., Niu Y., Zhang K. *The Corrosion of Various Materials Under Chloride Deposits at 623-723 K in Pure Oxygen.* High Temperature Materials and Processes 21 (2002) 11-24.

[94] Pérez F. J., Nieto J., Trilleros J. A., Hiero M. P. *Hot Corrosion Monitoring of Waste Incineration Processes Using Electrochemical Techniques.* Mater Science Forum 522-523 (2006) 531-538.

[95] Otero E., Pardo A., Pérez F. J., Utrilla M. V., Levi T. *Corrosion Behaviour of 12CrMoV Steel in Waste Incineration Environments: Hot Corrosion by Molten Chlorides*. Oxid Met 51, Nos. 5/6 (1999).

[96] Otero E., Pardo A., Merino M. C., Utrilla M. V., López M. D., Peso J. L. *Corrosion Behaviour of IN-800 Superalloy in Waste Incineration Environments: Hot Corrosion by Molten Chlorides.* Oxid Met 49, Nos. 5/6 (1998).

[97] Ruh A., Spiegel M. *Thermodynamic and kinetic consideration on the corrosion of Fe, Ni and Cr beneath a molten KCl-$ZnCl_2$ mixture.* Corros Sci 48 (2006) 679-695

[98] Spiegel M. *Corrosion Mechanisms and Failure Cases in Waste Incineration Plants.* Mater Sci Forum 369-372 (2001) 971-978.

[99] Nakagawa K., Matsunaga Y. *The effect of Chemical Composition of Ash Deposit on the Corrosion of Boiler Tubes in Waste Incinerators.* Mater Sci Forum 252-254 (1997) 535-542.

[100] Westén-Karlsson *Assessment of a Laboratory Method for Studying High-temperature corrosion Caused by Alkali Salts.* Lic. Thesis, Åbo Akademi University, Åbo, Finland (2008).

[101] Watt I. M. *The principles and practice of electron microscopy.* Cambridge University Press (1985), ISBN: 0-521-25557-0.

[102] Thermo Scientific Xphase NORAN System 7 http://www.thermo.com/eThermo/CMA/PDFs/Articles/articlesFile_7108.pdf (accessed November 22, 2011).

[103] Laurén T. *Methods and Instruments for Characterizing Deposit Buildup on Heat Exchangers in Combustion Plants*. Lic. Thesis, Åbo Akademi University, Åbo, Finland (2007).

[104] http://dekati.com/cms/dlpi (accessed March 22, 2012).

[105] Bale C. W., Bélisle E., Chartrand P., Decterov S. A., Eriksson G., Hack K., Jung I.-H., Kang J.-B., Melançon J., Pelton A. D., Robelin C., Petersen S. *FactSage thermochemical software and databases - recent developments.* CALPHAD: Computer Coupling of Phase Diagrams and Thermochemistry 33 (2009) 295-311.

[106] SGTE - Scientific Group Thermodata Europe. http://www.met.kth.se/sgte/ (accessed November 22, 2011).

[107] Dinsdale A. T. *SGTE data for pure elements.* Calphad 15 (1991) 317-425.

[108] Li Y. S., Sánchez-Pastén M., Spiegel M. *High Temperature Interaction of Pure Cr with KCl.* Mater Sci Forum, 461-464 (2004) 1047-1054.

[109] Pettersson J. *Alkali Induced High-temperature corrosion of Stainless Steel*. Academic Dissertation, Chalmers University of Technology, Göteburg, Sweden (2008).

[110] Lehmusto J., Yrjas P., Skrifvars B-J., Hupa M. *Detailed Studies on the High-temperature corrosion Reactions between Potassium Chloride and Metallic Chromium*. Mater Sci Forum 696 (2011) 218.

[111] Ma H. T., Wang L., Li Y. S., Zhao J. *Effect of $ZnCl_2$ vapor on high temperature oxidation of pure chromium.* J Mater Sci Lett 22, (2003) 763-765.

[112] Ugai Ya. A., Shatillo V. A. *The polytherm of the ternary system zinc chloride-lead chloride-potassium chloride.* J Phys Chem-U.S.S.R. 23 (1949) 744-54.

[113] Dombrovskaya N. S. *Double decomposition in the absence of a solvent. XXXIV. Reversible reciprocal system of potassium and lead chlorides and sulfates.* Izvestiya Sektora Fiziko-Khimicheskogo Analiza, Institut Obshchei i Neorganicheskoi Khimii, Akademiya Nauk SSSR 11 (1938) 135-150.

[114] Zhuang Y., Chen C., Timpe R., Pavlish J. *Investigations on bromine corrosion associated with mercury control technologies in coal flue gas.* Fuel 88 (2009) 1692-1697.

[115] Zahs A., Spiegel M., Grabke H. J. *Chloridation and oxidation of iron, chromium, nickel and their alloys in chloridizing and oxidizing atmospheres at 400-700 °C*, Corros Sci 42 (2000) 1093-1122.

[116] Jermer J.; Ekvall A.; Tullin C. *Inventory of contaminants in waste wood.* Värmeforsk Rapport 732; Värmeforsk: Stockholm, Sweden, 2001 (in Swedish).

[117] Robelin C., Chartrand P. *Therodynamic evaluation and optimization of the ($NaCl + KCl + MgCl_2 + CaCl_2 + ZnCl_2$) systems.* J Chem Thermodyn 2011, 43, 377–391.

RECENT REPORTS FROM THE COMBUSTION AND MATERIALS CHEMISTRY GROUP OF THE ÅBO AKADEMI PROCESS CHEMISTRY CENTRE:

06-01	Edgardo Coda Zabetta	Gas-Phase Detailed Chemistry Kinetic Mechanism "ÅA". A Mechanism for Simulating Biomass Conversion Including Methanol and Nitrogen Pollutants -Validation, Verification and Parametric Tests
06-02	Mischa Theis	Interaction of Biomass Fly Ashes with Different Fouling Tendencies
06-03	Michal Glazer	TGA-Investigation of KCl-Kaolinite Interaction
07-01	Vesna Barišić	Catalytic Reactions of N2O and NO over Bed Materials from Multi-fuel Circulating Fluidized Bed Combustion
07-02	Andrius Gudzinskas Johan Lindholm Patrik Yrjas	Sulphation of Solid KCl
07-03	Daniel Lindberg	Thermochemistry and Melting Properties of Alkali Salt Mixtures in Black Liquor Conversion Processes
07-04	Linda Fröberg	Factors Affecting Raw Glaze Properties
07-05	Tor Laurén	Methods and Instruments for Characterizing Deposit Buildup on Heat Exchangers in Combustion Plants
08-01	Erik Vedel	Predicting the Properties of Bioactive Glasses
08-02	Tarja Talonen	Chemical Equilibria of Heavy Metals in Waste Incineration -Comparison of Thermodynamic Databases-
08-03	Micaela Westén-Karlsson	Assessment of a Laboratory Method for Studying High Temperature Corrosion Caused by Alkali Salts
08-04	Zhang Di	*In vitro* Characterization of Bioactive Glass
08-05	Maria Zevenhoven, Mikko Hupa	The Environmental Impact and Cost Efficiency of Combustible Waste Utilisation - The Potential and Difficulties of Ongoing Technology Developments-
08-06	Johan Werkelin	Ash-forming Elements and their Chemical Forms in Woody Biomass Fuels
08-07	Hanna Arstila	Crystallization Characteristics of Bioactive Glasses

RECENT REPORTS FROM THE COMBUSTION AND MATERIALS CHEMISTRY GROUP OF THE ÅBO AKADEMI PROCESS CHEMISTRY CENTRE:

10-01	Markus Engblom	Modelling and Field Observations of Char Bed Processes in Black Liquor Recovery Boilers
11-01	Leena Varila *et al.*	Fyrtio år oorganisk kemi vid Åbo Akademi
11-02	Johan Lindholm	On Experimental Techniques for Testing Flame Retardants in Polymers
11-03	Minna Piispanen	Characterization of Functional Coatings on Ceramic Surfaces
11-04	Sonja Enestam	Corrosivity of hot flue gases in the fluidized bed combustion of recovered waste wood
12-01	Xiaoju Wang	Enzyme Electrode Configurations: for Application in Biofuel Cells
12-02	Patrycja Piotrowska	Combustion Properties of Biomass Residues Rich in Phosphorus

PROCESS CHEMISTRY CENTRE

ISSN 159-8205
ISBN 978-952-12-2746-2 (paper version)
ISBN 978-952-12-2747-9 (pdf version)
Painosalama Oy
Åbo, Finland, 2012